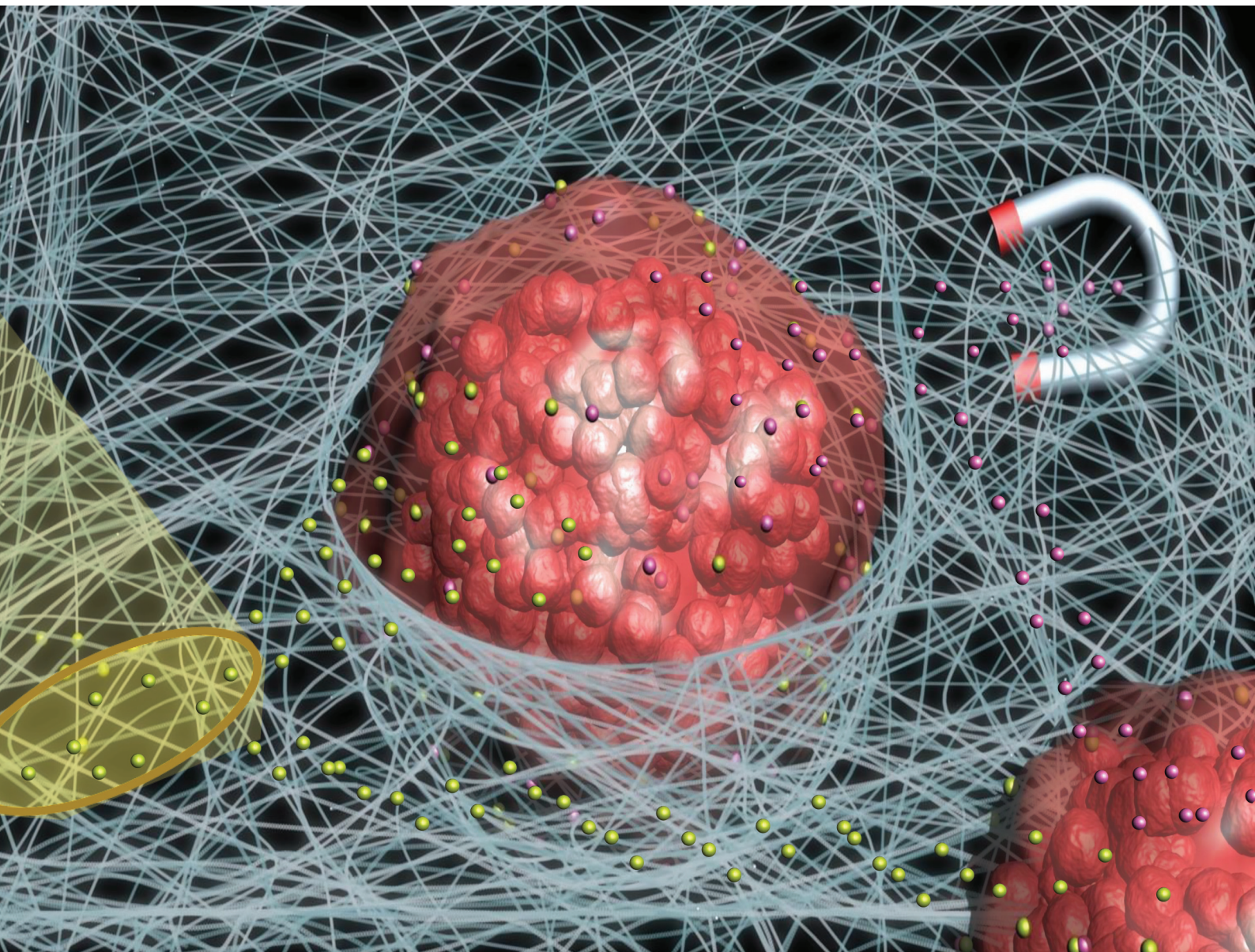


# Biomaterials Science

Volume 8  
Number 18  
21 September 2020  
Pages 4877-5220

[rsc.li/biomaterials-science](https://rsc.li/biomaterials-science)



ISSN 2047-4849


**REVIEW ARTICLE**

Loretta L. del Mercato *et al.*  
Electrospun nanofibers in cancer research: from engineering  
of *in vitro* 3D cancer models to therapy



Cite this: *Biomater. Sci.*, 2020, **8**, 4887

## Electrospun nanofibers in cancer research: from engineering of *in vitro* 3D cancer models to therapy

Marta Cavo,<sup>†a</sup> Francesca Serio,<sup>†a,b</sup> Narendra R. Kale,<sup>c</sup> Eliana D'Amone,<sup>a</sup> Giuseppe Gigli<sup>a,b</sup> and Loretta L. del Mercato  <sup>★a</sup>

Electrospinning is historically related to tissue engineering due to its ability to produce nano-/microscale fibrous materials with mechanical and functional properties that are extremely similar to those of the extracellular matrix of living tissues. The general interest in electrospun fibrous matrices has recently expanded to cancer research both as scaffolds for *in vitro* cancer modelling and as patches for *in vivo* therapeutic delivery. In this review, we examine electrospinning by providing a brief description of the process and overview of most materials used in this process, discussing the effect of changing the process parameters on fiber conformations and assemblies. Then, we describe two different applications of electrospinning in service of cancer research: firstly, as three-dimensional (3D) fibrous materials for generating *in vitro* pre-clinical cancer models; and secondly, as patches encapsulating anticancer agents for *in vivo* delivery.

Received 10th March 2020,  
Accepted 6th June 2020  
DOI: 10.1039/d0bm00390e  
rsc.li/biomaterials-science

### 1. Introduction

Electrospinning (ES) is a worldwide recognized process to produce fibrous and porous two-dimensional (2D) and three-dimensional (3D) materials starting from a polymeric solution.<sup>1–4</sup> The success of ES is mainly related to its versatility, despite being a simple and cost-effective technique: during the ES process, an electrified polymeric jet experiences bending instability and solidifies to produce long and continu-

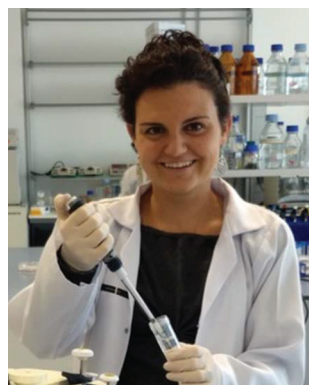
<sup>a</sup>Institute of Nanotechnology, National Research Council (CNR-NANOTEC), c/o Campus Ecotekne, via Monteroni, 73100 Lecce, Italy.

E-mail: [loretta.delmercato@nanotec.cnr.it](mailto:loretta.delmercato@nanotec.cnr.it)

<sup>b</sup>Department of Mathematics and Physics “Ennio De Giorgi”, University of Salento, via Arnesano, 73100 Lecce, Italy

<sup>c</sup>MIT-WPU, School of Pharmacy, Kothrud, Pune 411038, India

<sup>†</sup>These authors contributed equally.



**Marta Cavo**

Marta Cavo obtained her MSc degree in Biomedical Engineering in 2014 from the University of Genoa (Italy) and her PhD in Bioengineering in 2018 from the same university, with a thesis on the development of bioengineering models and tools (bioreactors) to support cancer research. During PhD she collaborated with CNR-IEIT (Genoa) and the University of Basel (CH). She is currently a postdoctoral Research Fellow at

CNR-NANOTEC (Lecce, Italy). Her main research interests include the development of novel 3D *in vitro* cancer models based on spheroids, hydrogels and sensing tools, to be used as *in vitro* platforms for anti-cancer compound screening.



**Francesca Serio**

Francesca Serio obtained her MSc degree in Nanobiotechnologies and Medical Biotechnologies in 2015 from the University of Salento (Lecce, Italy) and her PhD degree in Physics and Nanosciences in 2019 from the University of Salento (Lecce, Italy). She is currently a postdoctoral Research Fellow at the CNR Institute of Nanotechnology (Lecce, Italy). Her main research interests include synthesis and validation of stimuli-responsive

electrospun fiber architectures for tissue engineering and drug delivery applications.



ous nanofibers with diameters ranging from a few tens of nanometers to a few micrometers.<sup>5</sup>

ES has been significantly used for tissue engineering (TE) applications, since a huge number of different structures, morphologies and compositions can be obtained and adopted to make fibers suitable for vascular, bone, neural, tendon and ligament regeneration.<sup>6–14</sup> In particular, a lot of studies have been published in the field of bone regeneration, where a nanofibrous substratum provides favourable conditions for bone-associated cell anchorage and growth;<sup>15,16</sup> the random nature of fiber deposition produces the surface roughness suitable for cell attachment in bone scaffolds, as well as for osteoblastic differentiation and mineralization that are better regulated on nanofibrous surfaces than on more dense structures.<sup>17</sup> ECM-like electrospun structures are also suitable for muscle cell adhesion, since myoblast cells require highly aligned (anisotropic) or unidirectionally oriented fibers to adhere and proliferate.<sup>18,19</sup> The use of electrospun scaffolds as substrates for neural tissue engineering was also investigated; in this context, several groups have demonstrated how electrospun fibers show great efficacy in enhancing nerve regeneration.<sup>20,21</sup> Last but not least, electrospinning has been used to produce thin tubes to be used as scaffolds to make blood vessels.<sup>22–26</sup>

In cancer treatment, nanofibers have many advantages such as the ability to obtain fibers with diameters ranging from nanometers to sub-micrometers, surface modification, alignment variation and drug encapsulation. Anticancer drug loaded ES nanofibers enable controlled and sustained drug release at the desired site of action with improved efficacy. ES nanofibers have also been used as an implant into a post-operative tumour cavity, to inhibit tumour recurrence and to prolong drug release at the tumour site.<sup>27</sup> Furthermore, ES nanofibers provide a unique opportunity to build cell environments which can mimic the *in vivo* tumour micro-environ-

ment.<sup>28</sup> Some of the recent studies towards 3D *in vitro* cancer model development are mentioned below.

Over the last few years, the research community has focused on the possibility to translate tissue engineering principles and methods into cancer research, with the aim to provide physiologically relevant 3D *in vitro* cancer models. This new branch is known as cancer tissue engineering and aims to explore cancer pathogenesis and evolution in a more realistic environment than 2D cultures or animal models.<sup>29–31</sup> In this context, also the electrospinning technique has been repurposed to obtain 3D fibrous materials with properties similar to those found in native tumours.<sup>32</sup> At the same time, in the last few years, electrospun matrices have gained attention also in clinical applications: thanks to their porous structure and ability to incorporate drugs within the fiber lumen, electrospun fiber matrices have been used as a transdermal drug delivery system (TDDS) to facilitate delivery through skin in a controlled way; this application is particularly relevant in the case of anticancer treatments that are often associated with several drawbacks, such as poor solubility and instability in the biological environment, adverse effects on healthy tissues and low concentration at tumour sites.<sup>33</sup> We have listed some of the polymers used for anticancer drug delivery *in vitro* analysis using cancer cell lines (Table 1).

However, there are a few challenges in ES nanofiber applications such as achieving uniform drug distribution in ES fibers and drug compatibility in polymer solutions, avoiding initial burst release of drugs, and developing 3D scaffolds with desired porosity. Due to these critical parameters, all the electrospun nanofiber-based systems for cancer research are still in preclinical trials only. We discuss ahead the challenging parameters of ES fibers in cancer research.

All these facts highlight the multiple applications of electrospinning to solve the problems encountered in cancer research. The first part of this review will be dedicated to the



**Narendra R. Kale**

*Narendra Kale has submitted his PhD Thesis in Pharmaceutics at Savitribai Phule Pune University under the supervision of Prof. Jayant Khandare. His PhD studies involved the evaluation of cellular responses using anti-cancer drug delivery systems. His research involves the design and synthesis of nanomaterial substrates and in vitro evaluation for morphological alterations using cancer cells. He is currently a Research Scientist at*

*Actorius Innovation and Research, India. His current project involves the application of morphological traits for early diagnosis and identification of Circulating Tumor Cells from the blood samples of cancer patients.*



**Eliana D'Amone**

*Eliana D'Amone obtained her Diploma in chemical biology in 1999. She is a laboratory technician at the CNR Institute of Nanotechnology (Lecce, Italy). Her research activities are focused on the nano- and micro-fabrication of biomaterials, characterization by means of electron and fluorescence microscopy, and preparation of 2D and 3D cell cultures.*



**Table 1** List of polymers used for *in vitro* anticancer drug delivery studies

Polymer	Fiber diameter	Drug	Cancer type	Ref.
PLGA	430 nm	Doxorubicin hydrochloride and camptothecin	HepG-2 cells (human liver cancer)	34
PLLA	300 nm	5-Fluorouracil and oxaliplatin	Colorectal cancer	35
PEG-PLLA	690 nm	Carmustine	Glioma C6 cells	36
PCL	80–120 nm	5-Fluorouracil and paclitaxel	TNBC cells (human triple negative breast cancer)	37
pNIPAM	600–800 nm	Doxorubicin	Hela cells (human cervical cancer)	38
PVA	260 nm	Doxorubicin	SKOV3 cells (ovary cancer)	39

Abbreviations: PLGA – poly lactic-*co*-glycolic acid, PLLA – poly(L-lactic acid), PEG-PLLA-poly(ethylene glycol)-poly(L-lactic acid), PCL – poly( $\epsilon$ -caprolactone), pNIPAM – poly(*N*-isopropylacrylamide), and PVA – poly(vinyl alcohol).

summarization of the state of the art electrospinning-based 3D *in vitro* tumour models, subdivided according to the type of cancer studied or as membranes for intra- and extravasation studies; the second part will review the clinical applications of electrospun fibers for local therapy, giving overall a complete picture of electrospinning meeting cancer research, both *in vitro* and *in vivo*.

## 2. Overview of the electrospinning technique

Electrospinning is basically an electro-hydrodynamic phenomenon: it begins with the exposure of a charged polymer to an electric field between a metal needle and a collector; this causes instability within the polymer solution that deforms the spherical droplet to a conical shape (Taylor cone); at this stage, ultrafine fibers are extruded from the conical polymer droplet, and are collected on a metallic collector kept at an optimized distance.<sup>6,40,41</sup> The fiber formation process begins with jet initiation followed by jet whipping instability. A stable charged jet initiates when the applied voltage exceeds a critical value and the electrostatic force overcomes the fluid surface

tension. Charge forces cause the whipping of the liquid jet towards the collector, allowing the polymer jet to stretch up to a diameter of a few nanometers. During this process, the jet shows non-axisymmetric (with reference to the jet center line) instabilities, *i.e.* bending instability and axisymmetric instability *i.e.* Rayleigh instability. Rayleigh instability is observed in the presence of two opposing forces on the surface area, *i.e.* the surface tension and electrostatic repulsion of charges in the jet.<sup>5,42</sup> To successfully complete this process, ES apparatus has to be composed of a high voltage source (1–30 kV), a syringe pump to extrude the solution at a defined flow rate, a metallic needle and a conductive collector.<sup>41,43,44</sup> The electrospinning process begins with sufficiently high electrostatic force generated by the increased applied voltage. The applied voltage is inversely proportional to the fiber diameter because of enhanced fiber stretching due to the higher voltage. In addition to the applied voltage, the viscosity of the solution plays a crucial role in the ES process. If low viscosity fluid is used, the solution cannot resist Rayleigh instability and break up into droplets. If the viscosity of the fluid is sufficiently high with long chain molecule content, the solution can withstand against Rayleigh instability and the fluid jet leads to nanofibers deposited on the collector.<sup>45,46</sup>



**Giuseppe Gigli**

*Giuseppe Gigli is a Full Professor at the University of Salento (Lecce, Italy). He is the founder and Director of the CNR Institute of Nanotechnology, where he is also a coordinator of the Molecular Nanotechnology group. He is a member of the European Laboratory of Nonlinear Spectroscopy (LENS) Scientific Board, a member of the Administration Board of the High-Tech District (DHITECH) and a coordinator of the*

*Precision Medicine Technopole in Lecce. His main research activities involve the study and fabrication of organic optoelectronic/photonic devices, microfluidic laboratories on a chip and drug delivery systems for advanced theranostics.*



**Loretta L. del Mercato**

*Loretta L. del Mercato obtained her MSc degree in Biotechnology in 2004 from University “Federico II” of Naples (Italy) and her PhD degree in Nanotechnology in 2017 from the ISUFI School at the University of Salento in Lecce (Italy). At present, she is a Senior Researcher at the CNR Institute of Nanotechnology and a coordinator of the “3DCellSensing” group. Currently, her research interests are mainly focused on*

*the synthesis and optimization of multifunctional (bio)materials for biosensing and therapy, with an emphasis on personalized cancer treatment strategies.*



Solvent evaporation plays a major role while the fluid jet flies towards the collector under the influence of electrostatic force. Solvent evaporation from the fluid jet occurs prior to obtaining a dry nanofiber deposited on the collector. There should be an optimum collecting distance, flow rate and viscosity of solution which are sufficient for solvent evaporation and fiber stretching. Decreased collecting distance and increased flow rate and viscosity result in non-evaporation of the solvent, which leads to bead like structures or an increased nanofiber diameter. Interplay among the applied voltage, solution viscosity, collecting distance, solvent evaporation and flow rate take place during the ES process and to obtain the desired nanofiber characteristics, it is necessary to optimize these parameters. Solvent selection is another critical parameter during the ES process. Highly volatile solvents may cause jet drying at the tip of the needle because of a low boiling point. Meanwhile, less volatile solvents can result in insufficient drying of the fluid jet and poor fiber formation. If the polymer dissolves in two solvents, one as the solvent and another as the non-solvent, ES leads to highly porous nanofibers.<sup>47–49</sup>

Although it appears at first as an easy method, the entire process depends on a multitude of parameters, such as environmental parameters (temperature and humidity), solution properties (viscosity, conductivity and surface tension) and governing variables (distance between the tip and the collector, electric potential, flow rate, selected polymers, and geometry of the collector). All these parameters can affect the capacity of the spinneret, or the fiber and pore diameters or the structure and morphology of the fibers. Notably, through the optimization of the cited parameters, fibers can be obtained randomly or in an ordered way, larger or thinner, with or without beads.

### 2.1. Configurations for electrospinning

The two main principles implemented to achieve ES construction are as follows:

1. Manipulating the electric field *via* collector design (auxiliary electrodes):

Electrode arrangements and collector design had been varied to achieve better alignment of nanofibers. Parallel electrodes, multiple electrodes and charged pair electrodes had been tested to achieve the desired alignment of nanofibers. The use of a parallel electrode is one of the simplest ways to manipulate the electric field and drive the ES jet to swing back and forth between them, which leads to aligned fibers between the electrodes. The fiber should withhold its weight across the gap along with external electrostatic forces. A charged pair electrode has additional forces through alternate application of opposing charges. Alternate switching between charged electrodes causes the ES jet to bridge the gap between collector electrodes. For further improvement of the fiber alignment, steering electrodes were used simultaneously along with a parallel electrode collector.<sup>50,51</sup>

2. Moving the collector:

At the beginning, horizontal and vertical ES setups with flat collectors were proposed (Fig. 1a and b). Even though the grav-

itational force affecting the polymer is negligible with respect to the electric field forces, gravity has an effect on the shape of the polymer droplet and the Taylor cone; in particular, the shape of the droplet forming depends on the flatness of the needle tip; so in a vertical configuration the needle tip has to be straightened.<sup>52</sup> Besides that, the real revolution in ES occurred when it was discovered that the geometry of the collector could influence the arrangement of the fibers and, in particular, could allow obtaining aligned fibers instead of random ones. This result can be achieved by substituting the traditional flat collector with a rotating collector (Fig. 1c).

The purpose of the rotating collector is to mechanically stretch the fibers helping them to align along the collector. Collector configurations include a solid cylinder which can rotate about its axis, a conducting wire wound on an insulated cylinder, a wired drum or a disc collector (Fig. 2a–d). With this last configuration, double- and triple-layer highly aligned crossbar structures were obtained.<sup>53</sup>

Also in the case of rotating collectors, the alignment of fibers can be optimized by varying several parameters such as polymer viscosity and rotational speed, or improving the set-up with two oppositely placed needles as shown by Pan *et al.*<sup>54</sup> In this work, fibers coming out of the two needles combined in a yarn, which was wound by a cylinder collector rotating at a high speed. Fibers manufactured by this method were continuous, well-aligned, and could be deposited over a large area; moreover, increasing the velocity improved the alignment of the fibers (Fig. 2e and f).

### 2.2. Materials

So far, more than fifty different polymers and solvents have been successfully electrospun into fibers with diameters in the range from 3 nm to 1 mm. The interactions between the solvent and polymer have been found to be crucial in ensuring a successful production of continuous nanofibers.<sup>55</sup> In addition, the solvent selection is important for solution conductivity and may affect the fiber size distribution.<sup>56</sup>

Substantially, the material choice depends on the application of the scaffold. For TE purposes, the choice is based on the properties of the tissue to be regenerated and biodegradable polymers are preferably used. The mostly synthetic materials used in TE are polyesters, such as poly(lactide) (PLA), poly(glycolide) (PGA) and poly(caprolactone) (PCL). Natural materials, such as cellulose, collagen, natural silk, fibrinogen, chitosan and hyaluronic acid, are of interest for use in regenerative medicine because the material becomes more recognizable for the cells.<sup>57</sup> However, not all these natural polymers can be easily used with ES: for example, processing chitosan with ES is difficult because of its polycationic nature and its high viscosity in solution, and toxic or highly acidic solvent is needed for electrospinning;<sup>58</sup> again, gelatin is not stable if electrospun as a single material; finally, hyaluronic acid solutions have very high viscosity and consequently producing uniform fibers from them can be difficult.<sup>59</sup>

The available literature in this field demonstrates the ability to electrospin natural polymers with the possibility to exploit



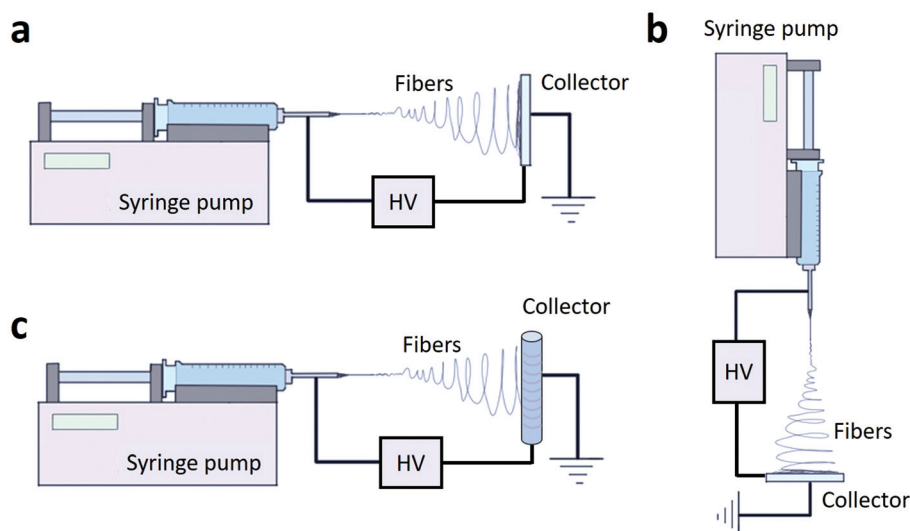


Fig. 1 Different configurations of the ES set-up: horizontal (a), vertical (b) and with a rotating collector (c).

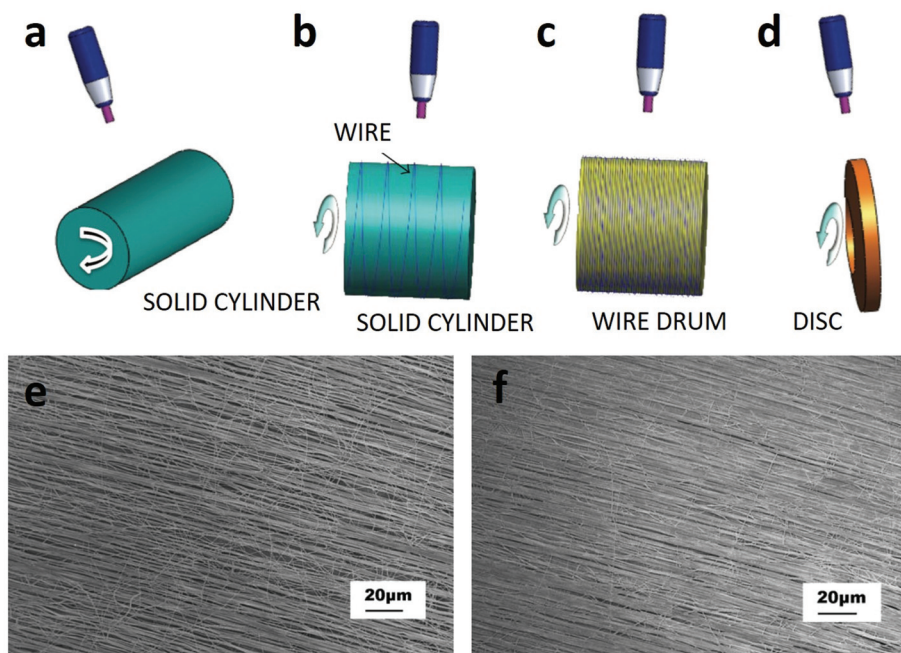


Fig. 2 Category of ES set-ups based on the rotating device. These configurations include (a) a solid cylinder, (b) a wire wound on an insulated cylinder, (c) a wired drum, and (d) a disc collector.<sup>53</sup> Well-aligned PVA fibers collected on a Teflon tube with different surface velocities: (e) about  $1.3 \text{ m s}^{-1}$  and (f)  $2.3 \text{ m s}^{-1}$ .<sup>54</sup> Reproduced from ref. 54 with permission from Elsevier, copyright 2006.

their biocompatibility.<sup>60</sup> However, when compared with synthetic materials, two main drawbacks such as poor mechanical performance and difficult electrospinnability are clear.

### 3. Electrospinning for 3D *in vitro* cancer models

Traditionally, cancer biology research has involved *in vitro* analysis of cell behaviour predominantly using two-dimensional

(2D) cell cultures and *in vivo* animal models:<sup>61</sup> in detail, 2D models are routinely used as initial systems for evaluating the effectiveness of molecules as potential therapeutic drugs; this initial screening precedes animal studies before advancing to human clinical trials.<sup>61</sup> The dissimilarities in cell behaviour between 2D cultures and real tumours are well known and they mainly derive from changes in gene expression originating from the different interactions to which the cells are subjected within a 2D microenvironment if compared to a more natural 3D microenvironment.<sup>62–70</sup> A striking example of this is rep-



**Table 2** List of nanofiber scaffolds used for the 3D culture technique with a noted difference of cell line behavior on 3D scaffolds than on 2D culture of the same material

3D nanofiber scaffolds	Fiber diameter	Cell line	Noted difference from 2D culture	Ref.
PCL	400 nm to 2 $\mu$ m	CT26 colon cancer cells and bone marrow-derived dendritic cells (BM-DC)	Lipopolysaccharide (LPS)-activated BM-DCs showed increased expression of CD86 and major histocompatibility complex class II	76
PEG	<600 nm	NIH 3T3 cells	Five times higher cell proliferation	77
PCL	295–701 nm	Triple negative breast cancer (TNBC) cells	Higher mammosphere forming capacity and aldehyde dehydrogenase activity, higher cell proliferation and elongation	78
	—	Ewing sarcoma cells	More resistant to traditional cytotoxic drugs, also exhibited remarkable differences in the expression pattern of the insulin-like growth factor-1 receptor/mammalian target of the rapamycin pathway	79
Silk	497 nm	HN12 cells	Increased paclitaxel drug concentration in order to achieve a cytotoxic effect	80
PVA and PEOT	5–10 $\mu$ m	Pancreatic ductal adenocarcinoma cells (PDAC)	Primary PDAC cells showed good viability and synthesized tumour-specific metalloproteinases (MMPs) such as MMP-2, and MMP-9	81
PDMS and PMMA	1.15–3.6 $\mu$ m	Human lung cancer epithelial cells (A549)	Leads to the formation of cell spheroids from single cells	82

Abbreviations: PCL – poly( $\epsilon$ -caprolactone), PEG – poly(ethylene glycol), PCL – poly( $\epsilon$ -caprolactone), PVA – poly(vinyl alcohol), PEOT – poly(ethylene oxide terephthalate), PDMS – poly(dimethyl siloxane), and PMMA – poly(methylmethacrylate).

resented by the unequal nutrient concentration to which cells are exposed: in 2D cultures, cells are uniformly exposed to nutrients, while *in vivo* the concentration of soluble factors influencing cell proliferation is characterized by spatial gradients that play a vital role in biological differentiation, organ development and countless other biological processes.<sup>71–74</sup> Cancer cells would alter their behaviour in 2D culture from their *in vivo* behaviour. However, 3D scaffolds will mimic *in vivo* conditions which will help in precise analysis of the cellular response against anticancer drugs. It is therefore not surprising that many aspects of tumorigenesis are still not fully understood.<sup>75</sup> Below, we have listed noted differences of cell line behaviour on 3D scaffolds from that on 2D culture of the same material (Table 2).

On the other side, there is a growing awareness of the limitations of animal research and its inability to make reliable predictions for human clinical trials. Indeed, animal studies seem to overestimate by about 30% the likelihood that a treatment will be effective because negative results are often unpublished.<sup>83</sup> For all these reasons there is growing interest in developing new 3D *in vitro* cancer models to be adopted as pre-screening models and to recapitulate the 3D microenvironment where cancer cells live.

### 3.1. Electrospun fibers as extracellular matrix (ECM)-like materials to mimic the cancer microenvironment

Cancer cells within a solid tumour are in close contact with the ECM, which is mainly composed of collagen, fibronectin, elastin, laminin and proteoglycan<sup>84,85</sup> with additional components for specific tissues.<sup>86</sup> In a pathological environment such as the cancer one, the ECM cannot be considered just as a passive environment surrounding cells, but as an active component with a critical role in regulating tumour cell properties and behaviour.<sup>87</sup> Specifically, in breast cancer, the ECM

stiffness affects cancer development and migration;<sup>73,88,89</sup> in ovarian cancer patients, the expression of collagen VI correlates with the tumour grade and it has been shown to be upregulated in drug-resistant cancer cells, which can subsequently remodel the ECM to further promote chemoresistance;<sup>90</sup> again, in small cell lung cancer (SCLC) the adhesion of cancer cells to the ECM enhances tumorigenicity and confers resistance to chemotherapeutic agents.<sup>91</sup> Ideally, a 3D tumour model should be able to recapitulate this cell–ECM crosstalk. In order to study the ECM–cancer cell interactions in a 3D environment, biomimetic substrates have been produced.<sup>92</sup> A number of strategies exist, and above all Matrigel, a commercial basement membrane preparation, is used.<sup>93–95</sup> Besides that, a lot of 3D scaffolds have been used to culture cancer cells *in vitro*, allowing for their growth and proliferation in a context closer to reality than 2D traditional cultures. Electrospun fiber scaffolds provide an effective artificial 3D culture matrix due to their biomimicry of the architecture of the ECM<sup>96,97</sup> and high versatility in biochemical stimuli, including growth factors, adhesion molecules, and drugs.<sup>60,98</sup> In the following paragraphs, we will analyse the state of the art *in vitro* 3D tumour models with a focus on electrospun micro- and nanofibres, citing some of the most relevant works in the field. The paragraphs have been subdivided according to the cancer type.

**3.1.1. Breast cancer.** Breast cancer is the most common cancer in women across most ethnic groups and accounts for 30% of all new cancer diagnoses.<sup>99</sup> Consequently, its treatment has attracted a lot of interest. Among all the 3D *in vitro* breast cancer models proposed in the literature, some based on the ES technique showed very promising results. In 2012, Saha *et al.* created electrospun fibrous scaffolds of PCL dissolved in 1,1,1,3,3,3-hexafluoro-2-propanol (HFIP) with random and aligned fiber orientations in order to mimic the structure of



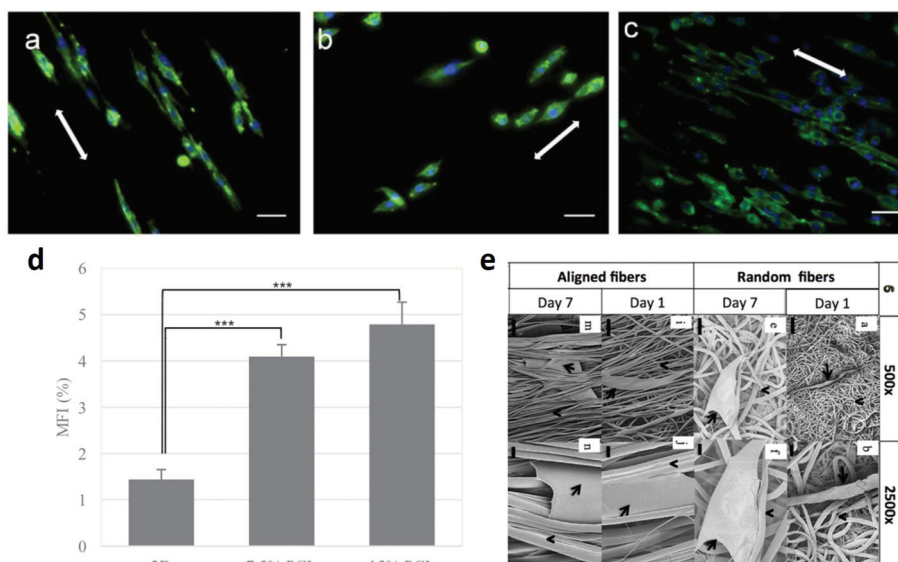


**Fig. 3** Response of different breast cancer cell lines on aligned PCL fibers: (a) 4T1, (b) MTCL, and (c) MDA-MB-231. Cells were cultured on PCL fibers for 3 days. Green represents the actin cytoskeleton and blue the nucleus of a cell, scale bar = 40  $\mu\text{m}$ .<sup>98</sup> (d) Mammosphere forming index (MFI) of MCF-7 cells after 2D and 3D culture on electrospun scaffolds. Statistically significant level was  $p < 0.001$ .<sup>102</sup> (e) SEM images of MDA-MB-231 cells on fibrous scaffolds after day 1 and day 7 of culture. The arrows depict the cell body and the arrowheads depict the fibers.<sup>101</sup> Reproduced from ref. 98 with permission from John Wiley and Sons, copyright 2017, and ref. 102 with permission from Elsevier, copyright 2011.

the ECM; the human breast cancer cell line MCF-7 was cultured on fibrous scaffolds for 3–5 days, showing an elongated morphology in the aligned fibers and maintaining a mostly flat stellar shape in the random fibers, demonstrating how the topographical cue may play a significant role in tumour progression.<sup>100</sup> In a different work, Girard and colleagues showed that 3D scaffolds prepared by ES promoted cancer cell growth in irregular aggregates similar to *in vivo* tumoroids with epithelial to mesenchymal transition (EMT) induction, as shown by upregulation of vimentin and loss of E-cadherin expression (Fig. 3).<sup>101</sup> In another work by Du *et al.*, the expression of the adhesion-related genes in human breast cancer cells cultured in electrospun nanofibrous scaffolds was time-dependent (Fig. 3).<sup>84,102</sup> In 2015, Guiro *et al.* fabricated scaffolds made of poly( $\epsilon$ -caprolactone) (PCL) having aligned or random fibers. Proliferation, viability and cell cycle analyses of breast cancer cells seeded on these substrates indicated that this 3D culture system prompted the more aggressive cells to adopt a dormant phenotype. The findings indicate that random and aligned fibrous PCL scaffolds may provide a useful system to study how the 3D microenvironment affects the behaviour of breast cancer cells.<sup>103</sup> In 2017, Rabionet *et al.* fabricated ES scaffolds from different PCL-acetone solutions. PCL meshes were seeded with triple negative breast cancer (TNBC) cells. Notably, under the tested conditions, cells exhibited a higher mammosphere forming capacity and aldehyde dehydrogenase activity than 2D cultured cells.<sup>78</sup>

**3.1.2. Pancreatic cancer.** Pancreatic ductal adenocarcinoma (PDAC) is a highly lethal neoplasm, with a 5-year survival rate of only 6%.<sup>104</sup> These mortality rates depend on several factors: a lack of diagnostic markers, a high degree of infiltration and

metastasis and strong resistance to conventional chemotherapy. Moreover, PDAC is characterized by a very heterogeneous and rich stroma, comprising cellular and extracellular matrix (ECM) components, which seems to play a crucial role in the inefficiency of chemotherapy.<sup>105</sup> For all these reasons, there is a strong need for new 3D *in vitro* PDAC models, even though few electrospinning-based models have been proposed. Among these, in 2013, He *et al.* successfully engineered a subcutaneous model using an electrospun scaffold<sup>106</sup> and, a few years later, the same group proposed a metastatic orthotopic pancreatic tumour model that recapitulated the tumour formation and hepatic metastasis (the landmark event of pancreatic cancer) by using a polyglyconate/gelatin electrospun scaffold. This metastatic tumour model showed an increased incidence of tumour formation, an accelerated tumorigenesis and a significant hepatic metastasis.<sup>107</sup> In 2014, Ricci and colleagues analysed the interactions of primary PDAC cells with different polymeric scaffolds, respectively, characterized by sponge-like pores *versus* nanofiber mesh interspaces, demonstrating that PDAC cells show diverse behaviours when interacting with different scaffold types that can be exploited to model various phases of pancreatic tumour development and invasion.<sup>81</sup>

**3.1.3. Colorectal cancer.** Electrospun fiber mats have been also exploited for providing preclinical 3D *in vitro* models of colorectal cancer, the third most common cancer among both men and women worldwide. In 2013, Yamaguchi *et al.* attempted to grow 3D cultures of various tumour cell lines, including human colon adenocarcinoma HT-29 and DLD-1 cells, on silicate fibers (SNFs) prepared by ES technology *via* a sol-gel process.<sup>108</sup> HT-29 and DLD-1 cells seeded on SNF



scaffolds grew gradually and formed tight aggregates showing a 3D cell morphology. Notably, cell viability assay for HT-29 cells showed a significantly increased drug resistance to mitomycin C in 3D cultures, likely because the drug penetration was restricted in the interior of the 3D structure, thus reducing the drug exposure in cells. Overall, the study demonstrated that SNF fibers obtained by ES technology could be used as an *in vitro* 3D tumour model for testing the efficacy of potential anticancer drugs. In 2016, Kim *et al.* explored electrospun mats made out of intertwined PCL nano- and submicron-scale fibers to grow 3D cocultures of colon cancer cells and dendritic cells. The authors reported the cocultures of mouse CT26 colon cancer cells and bone marrow-derived dendritic cells (BM-DCs) on PCL fibers characterized by efficient adhesion, spreading, and migration of top-seeded cancer cells and BM-DCs on the surfaces of the mats. In particular, they showed that PCL mats composed of a mixture of nanofibers with diameters ranging from 400 nm to 10  $\mu\text{m}$  permitted an optimal cell infiltration. Notably, BM-DCs cocultured on 3D PCL mats maintained their ability to sprout cytoplasm, to migrate, to synapse with and to engulf mitoxantrone-treated CT26 cancer cells, thus reproducing the *in vivo* cross-talk between these two cancer and immune cells.<sup>76</sup>

**3.1.4. Prostate cancer.** In 2009, Hartman *et al.* created electrospun micro- and nanofibrous collagen scaffolds to support prostate tumour growth in 3D. The effects of the matrix porosity, fiber diameter, elasticity and surface roughness on the growth of cancer cells were evaluated. The obtained data indicated that while cells attach and grow well on both nano- and microfibrillar electrospun membranes, and the microfibrillar membrane represented a better approximation of the tumour microenvironment. It was also observed that C4-2B non-adherent cells migrated through the depth of two electrospun membranes and formed colonies resembling tumours on day 3. An apoptosis study revealed that cells on electrospun substrates were more resistant to both anti-neoplastic agents, docetaxel (DOC) and camptothecin (CAM), compared to the cells grown on standard collagen-coated tissue culture polystyrene (TCP).<sup>32</sup>

**3.1.5. Ewing sarcoma.** Ewing sarcoma is a bone tumour mostly prevalent in adolescents and young adults, and it is rapidly fatal unless effectively treated.<sup>109</sup> Considering that most preclinical studies fail to predict whether a given drug candidate will work in clinical trials, in 2013, Fong *et al.* developed an *ex vivo* model based on PCL 3D mats, which conferred

a more physiologically relevant cell phenotype compared with traditional 2D cultures. Moreover, this model demonstrated pronounced upregulation of the insulin-like growth factor-1 receptor (IGF-1R) pathway, a receptor commonly expressed in Ewing sarcomas and one of the most promising targets in drug development phases.<sup>79</sup> Two years later, the same group improved the model to better mimic *in vivo* biology and drug sensitivity; in this work, Ewing sarcoma cells were seeded onto electrospun scaffolds in a flow perfusion bioreactor, where the fluidic shear stress could provide a physiologically relevant mechanical stimulation. They found that cells exposed to a fluidic flow produced more IGF1 ligands, demonstrating shear stress-dependent sensitivity to IGF-1 receptor targeted drugs as compared with static conditions. Moreover, flow perfusion increased nutrient supply, resulting in an enrichment of cell culture under static conditions (Fig. 4).<sup>110</sup>

**3.1.6. Glioblastoma.** Glioblastoma multiforme is the most aggressive and malignant brain tumour.<sup>111</sup> The available treatments are ineffective and some tumours remain inoperable because of their size or location. With the aim to advance the research in this field, in 2014 Jain *et al.* investigated the apoptosis of glioblastoma tumour induced by directional migration of tumour cells through the aligned fibers of an electrospun scaffold to a gel pool. It is difficult to treat brain cancer with current modalities due to drug delivery challenges at the desired site of action. However, if one could control tumour cell migration, it would be a useful approach in cancer therapeutics. Jain *et al.* demonstrated enhanced cell migration towards a cycloamine conjugated hydrogel sink, by using aligned nanofiber conduits. The results showed that these conduits with aligned fibers could promote the migration of glioma cells from the glioma tumour, finally providing an innovative method which may open up a new way for the application of electrospun fibers in the treatment of cancer.<sup>112</sup>

**3.1.7. Lung cancer.** In 2013, Girard *et al.* developed 3D nanofibrous scaffolds by ES a mixture of poly(lactic-co-glycolic acid) (PLGA) and a block copolymer of polylactic acid (PLA) and mono-methoxypolyethylene glycol (mPEG). The ability of cancer cells from different tumours to form aggregates on these scaffolds was investigated. Among these, LLC1 lung cancer cells were seeded on scaffolds and monitored for the morphology and cell viability. LLC1 cells when cultured on a 3P scaffold formed tumoroids at day three. The cells showed different characteristics in 3D scaffolds as compared to a

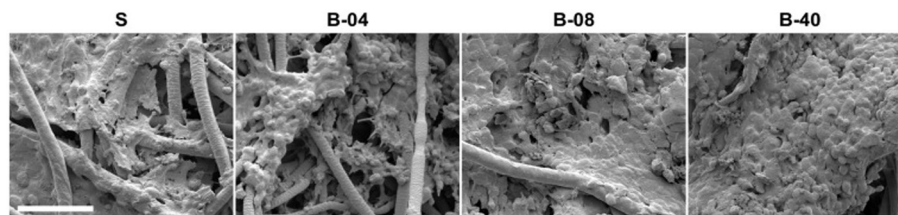


Fig. 4 SEM micrographs of Ewing sarcoma cell culture under static and flow perfusion conditions (S, static; B-04, 0.04  $\text{mL min}^{-1}$ ; B-08, 0.08  $\text{mL min}^{-1}$ ; and B-40, 0.40  $\text{mL min}^{-1}$ ). After 10 days of culture, scaffold surfaces for the different experimental groups were examined by SEM (scale bar, 50  $\mu\text{m}$ ).<sup>110</sup>



monolayer culture. 3D culture cells were more resistant to the anticancer drug along with upregulation of vimentin and loss of E-cadherin expression.<sup>101</sup>

**3.1.8. Bladder cancer.** Considering the proven critical role of the ECM in determining cell behaviour and tumour progression, in 2016 Alfano and colleagues performed a deep characterization of the healthy and tumoral human bladder ECM, finding the main features characterizing the tumoral one: (i) a loss of the tissue morphology, (ii) the linearization and degree of organization of fibrils of thin diameters and (iii) an increased vascularization. From these findings, the authors modelled a 3D synthetic bladder model able to create an environment more similar to the *in vivo* microenvironmental niche conditions to test innovative therapies. To this aim, they produced electrospun PCL-based scaffolds; the results showed that binding and invasion of the bladder metastatic cell line were observed on the synthetic scaffold recapitulating the anisotropy of the tumoral ECM, but not on the scaffold with a disorganized texture typical of non-neoplastic lamina propria.<sup>113</sup>

**3.1.9. Melanoma.** The incidence and mortality rates of melanoma, the most malignant skin cancer, have been rapidly growing in recent years,<sup>114</sup> but the effective management of this disease is still a challenge due to a lack of suitable culture systems. Trying to overcome this limitation, in 2017 Wang *et al.* developed a poly( $\gamma$ -benzyl-L-glutamate)/poly(lactic acid) (PBLG/PLA) electrospun membrane and demonstrated its suitability as a matrix for 3D culture of melanoma cells. In detail, their results show that – compared to other substrates – PBLG/PLA nanofiber membranes could better support cell viability and proliferation and, besides that, promoted the generation of tumoroid-like structures. These findings demonstrated that the proposed model could mimic the ECM of the melanoma microenvironment and could be a promising tool for 3D cell cultures.<sup>115</sup>

### 3.2. Electrospun fibers as membranes to study intra- and extravasation

All the 3D models presented in the previous section are promising in bridging the gap between *in vitro* and *in vivo* testing; however, they fail to mimic some specific and crucial steps of tumour evolution, including a cell motility and metastasis cascade. Considering the lethal impact of these mechanisms, there is a strong need to provide not only realistic *in vitro* models of primary tumours, but also reliable new models for intra- and extravasation, the two main phases of metastasis. The National Cancer Institute described extravasation as “the movement of cells out of a blood vessel into tissue during inflammation or metastasis (the spread of cancer)” and intravasation as “the movement of a cell or a foreign substance through the wall of a blood or lymph vessel into the vessel itself”. Cancer cells invade the stroma and metastasize to blood vessels as singlets or clusters. This stromal invasion is followed by extravasation into and intravasation from the blood vessels and subsequent invasion of neighbouring tissues. Invasive cells then re-establish distal colonies, causing metastasis.<sup>116</sup>

Thanks to their fibril structures, electrospun membranes have been proposed to mimic the tumour–blood vessel interface, the physical zones where intra- and extravasation take place, or specific zones where metastasis can occur, such as the bone. Some examples of hybrid systems are already present in the literature. For instance, Cavo and colleagues combined an alginate-Matrigel based gel with embedded breast cancer cells with electrospun membranes to examine the cell invasion capability; the results showed that the cells were able to migrate through the gels and attach to the membrane mimicking the vascular walls hosted within a bioreactor.<sup>72</sup> In a different work, Ali *et al.* successfully grew human bone-derived osteoblast cells onto electrospun PCL scaffolds to mimic the bone niche and integrated it into a bioengineered 3D *in vitro* model recapitulating prostate cancer metastasis to the bone.<sup>117</sup> Again, Rabionet *et al.* developed and used PCL scaffolds for 3D breast cancer cell culture by using ES nanofibers.<sup>78</sup>

Despite the little supporting literature, combining 3D tumour models with cellular infiltration throughout nanofiber scaffolds seems to be crucial for realizing completely engineered cancer models and to better recapitulate the microenvironment of cancer cells.

## 4. Electrospun nanofibrous devices for cancer therapy

Cancer treatment represents one of the most crucial issues in clinical management. Uncontrolled growth, immortality and the ability to metastasize are significant characteristics of cancer cells.<sup>118</sup> This paragraph aims to explore the existing applications of electrospun nanofibers in cancer therapy, mostly focusing on drug/gene delivery and cancer cell detection/sensing and highlighting the challenges and future directions for applications of electrospun nanofibers in cancer research.

### 4.1. Drug delivery

Conventional surgery, radiotherapy and chemotherapy are currently the most adapted treatment modalities for cancer.<sup>119</sup> However, these options are often limited and inadequate.<sup>120</sup> Actually, the clinical use of the most engaged chemotherapeutics against several solid and hematopoietic cancers, including breast cancer, osteosarcomas, aggressive lymphomas, and leukaemia, is usually limited by the severe and harmful side effects at therapeutic concentrations.<sup>63</sup> Moreover, in order to maximize the therapeutic effects, many patients need to take excess amounts of drugs, orally or *via* systematic injection, which might trigger side effects in healthy tissues.<sup>121</sup>

In order to limit the common systemic side effects and toxicity, researchers are currently focusing their work particularly on postoperative chemotherapy applications for developing innovative and sophisticated treatments to specifically target cancer cells.



Targeted microcarrier technologies such as micro- and nanoparticles, liposomes and nanofibrous materials are designed for drug delivery in a controlled manner to a specific site. The release of drugs in a controlled way is a complex challenge in which systems provide an optimal amount of the drug to a specific target at a predetermined rate and for a definite time period (ranging from days to years).<sup>122</sup>

Controlled release systems offer advantages when compared to conventional drug therapies. Firstly, they maintain the drug in the desired therapeutic range in the blood by a single administration and avoid oscillating drug levels attributed to the standard trend of injected drugs in the blood (the blood level of the drug rises, reaches a peak plasma level and then declines) which cause alternating periods of ineffectiveness and toxicity. Other advantages comprise the localized drug delivery to a specific target of the body. In this manner, one can guarantee an improvement of the pharmacological properties of free drugs and an increment of the patient compliance with a reduced amount of the needed drug and a decreased frequency of drug administration.<sup>122-124</sup> Moreover, in contrast to sustained release formulations, such as suspensions and emulsions, which are influenced by the environmental conditions and therefore are subjected to patient variations,<sup>122</sup> controlled release systems enable the drug to be preserved in a polymeric material. The release of the drug through the polymeric system network is controlled by two main mechanisms: (1) drug diffusion, which is the most common release mechanism, whereby the drug moves in a concentration gradient from the inner part to the system's outer side up to the body; and (2) chemical mechanisms, including the degradation of the polymer or the cleavage of the drug from a polymer linkage to allow the drug release.<sup>122</sup>

Electrospun fibers represent an ideal platform for drug delivery since they provide a high surface area to volume ratio and may favour abundant drug release.<sup>125</sup> Various delivery systems have been developed by loading antibiotics, anticancer drugs, proteins and also nucleic acids. The application of electrospun fibers for chemotherapy has become popular more recently, in particular as a local drug delivery system after a surgical operation for removing solid tumours.<sup>121</sup>

The active molecules can be (i) physically or chemically attached to the surface of the fibers or (ii) mixed with the polymers. In the following, the different loading methods will be presented.

**4.1.1. Drug loading.** Drug solubility in the polymer solution is decisive for selecting the right loading method. The drug loading method, for its part, plays a pivotal role in the release process. Generally, hydrophobic drugs such as doxorubicin and paclitaxel are well processed with organic solvents.<sup>126,127</sup> Hydrophilic drugs, such as peptides and proteins, are better handled in water-soluble polymers.<sup>128,129</sup> Here, the several possible routes for drug loading will be discussed.

The ES process with two or more constituents is one major approach to produce nanofibers encapsulating pharmaceuticals or other bioactive components with a significant drug

loading ability. This configuration requires the application of the conventional ES device (a single nozzle with a single capillary) in which both drugs and polymers are mixed together in the same solvent and then electrospun into drug-loaded fibers.<sup>130-133</sup>

Ranganath *et al.* reported the successful production of electrospun poly-(D,L-lactide-co-glycolide) fibers to deliver paclitaxel for postsurgical chemotherapy against malignant brain tumours. The device showed sustained paclitaxel release over 80 days *in vitro* and demonstrated tumour growth inhibition in an animal study.<sup>134</sup> Xu and co-workers developed an implantable biodegradable system for controlled release of a 1,3-bis(2-chloroethyl)-1-nitrosourea anticancer drug by ES a copolymer solution. The drug well dispersed through the polymer matrix and its release appeared directly proportional to the loaded drug amount.<sup>36</sup> Liu *et al.* designed biodegradable drug carriers for *in situ* treatment of liver cancer based on electrospun PLLA nanofibers loaded with doxorubicin hydrochloride in order to treat locally an unresectable liver cancer or to prevent a post-surgery tumour recurrence avoiding the systemic chemotherapy. The amount of doxorubicin hydrochloride loaded was completely released by diffusion from the nanofibers.<sup>135</sup>

Following this approach, Zong *et al.* developed an electrospun cisplatin-loaded delivery system to treat cervix cancer in mice *via* vaginal implantation. It showed a good mucoadhesive property and high anti-tumour power thanks to the cisplatin release from the nanofibers.<sup>136</sup>

Ramachandran *et al.* developed a localized nanoimplant for controlled delivery of the anti-cancer drug, temozolomide, in orthotopic brain-tumour. Specifically, a library of drug loaded (20 wt%) electrospun nanofibers of PLGA-PLA-PCL blends was produced with distinct *in vivo* brain-release kinetics (hours to months). Orthotopic rat glioma implanted wafers showed constant drug release (116.6  $\mu\text{g day}^{-1}$ ) with negligible leakage into peripheral blood (<100 ng) showing an ~1000-fold differential drug dosage in the tumour *versus* peripheral blood. Most importantly, an implant with a one-month release profile resulted in long-term (>4 month) survival in 85.7% animals, whereas a 7 day releasing implant showed tumour recurrence in 54.6% animals, exhibiting a median survival of only 74 days.<sup>137</sup>

However, ES is not immune to a few drawbacks. Above all, this method of synthesis leads to an initial burst release of the drug.<sup>130,138</sup> This is due to fast diffusional effects and probably it is predisposed by the low physical interactions between the drug and the polymer, so that, during the process, most of the drug molecules are likely to be localized around the fiber surface.<sup>130,139,140</sup> As a result, most of the drug amount came in contact with the surrounding water solution and this caused a subsequent large burst release at short times.<sup>139</sup> In addition, the burst release is often affected by the biodegradable feature of the chosen carrier.<sup>130-132,140</sup> Thus, a special caution is required to tailor both the release and the degradation rate, for example by varying the polymer blend composition and the ratio of amorphous to crystalline segments in order to control whether drug release occurs *via* diffusion alone or by diffusion and scaffold degradation.<sup>141,142</sup>



In contrast to ES, researchers have developed an original approach to limit the initial burst and, in this sense, to extend the drug release over a long period of time.

A good approach to prolong the therapeutic release of the drug from electrospun fibers is to add an inorganic nano-carrier into the fibers, such as silica based nanoparticles<sup>143–145</sup> and hydroxyapatite.<sup>146</sup>

For example, Zhou *et al.* implemented the conventional ES setup by firstly loading the anticancer doxorubicin drug into SiO<sub>2</sub> nanoparticles and then mixing the resulting solution with the polymer solution.<sup>143</sup> In the study of Zheng *et al.*, amoxicillin, a model drug, was adsorbed to the hydroxyapatite surface particles before to disperse them into PLGA solution ready to be electrospun. The model showed a sustained release profile and a limited initial burst release.<sup>146</sup> Moreover, novel drug carriers with a higher affinity for both drug molecules and polymer solution were then engaged. An example is the star polymer *ad hoc* synthesized in the work of Balakrishnana and co-workers which is optimal for further applications. The star polymer was blended with the more traditional PCL and the system was used for sustained release of doxorubicin.<sup>147</sup>

Another big issue in mixing the drug and polymer together is the exposition of drugs to harsh solvents, often necessary to dissolve the most used polymers. A range of biomolecules, including anti-cancer drugs, can be easily immobilized on the surface of electrospun fibers *via* a chemical or physical method for sustained drug delivery. This way of surface functionalization has at least two main advantages when compared to conventional ES. Firstly, physical and chemical drug immobilization after fiber synthesis can avoid the denaturation or inactivation of the drug generally caused by a high voltage or harsh organic solvents; secondly, the possibility to add additional materials after the ES process leads to avoiding of unexpected but usual trouble in terms of electrospinnability, for instance the difficulties in dissolving such biomolecules in an organic solvent because of their high molecular weight and the charges present on their surfaces.

Physical non-specific random adsorption is governed by electrostatic interactions, hydrophobic interactions, hydrogen bonding, and van der Waals interactions between drugs and the fiber surface.<sup>148</sup> However, non-specific adsorption allows the formation of weak links and it may favour a significant burst release. This is the reason why it is rarely used for anti-cancer therapy applications.

A more applied strategy is immobilization after chemical treatment of the fiber surface, by which it is possible to tailor fiber adhesion properties by adding appropriate functional groups such as amine, carboxyl, hydroxyl or thiol groups suitable for further immobilization.<sup>149</sup> Chemical conjugation methods are better for finely controlling the amount of the incorporated drug on the nanofiber mesh than physically trapping the drug on the surface, and they exhibit slow drug release kinetics with reduced initial burst release.<sup>150</sup> For instance, Volpato and co-workers reported a chemical immobilization of heparin-containing polyelectrolyte complex nanoparticles and a basic fibroblast growth factor onto chitosan

electrospun fibers. They prevented the burst release effect by post-fabrication modification of the fiber surface by adding a single bilayer of a polyelectrolyte multilayer composed of *N,N,N*-trimethyl chitosan and heparin.<sup>151</sup> Im *et al.* limited the initial burst by modifying cross-linked hydrogel fibers through fluorination before the addition of the model drug.<sup>152</sup> A versatile surface modification method is the approach performed by Ma *et al.* that worked on a porous nanofiber device made of a chitosan/polyethylene oxide mixture. After fabrication, the nanofibers were soaked in water to remove polyethylene oxide and then immersed in a solution with the anticancer drug to load it. Finally, the porous drug-loaded device was dipped in hyaluronic acid solution with the aim to control drug release thanks to the chitosan matrix and hyaluronic acid affinity.<sup>153</sup> The best promising strategy to limit the initial burst release is the use of core-shell fibers with coaxial needles.<sup>154–156</sup> The Coaxial ES technique has high potential in biomedical applications for core/sheath nanofibers since the polymer shell generally protects the core compounds from direct exposure to the external environment and, consequently, contributes to the prolonged drug release.<sup>157</sup> Coaxial ES is very useful mainly for the encapsulation of bioactive compounds which are susceptible to harsh organic solvents (drugs, proteins, cells and nucleic acids).<sup>155,156</sup> For instance, Zhang and collaborators demonstrated the successful loading of fluorescein isothiocyanate-conjugated bovine serum albumin, a model protein, in a water-soluble core of poly(ethylene glycol) within a PCL shell. These core-shell fibers showed a reduction of the initial burst release compared to fibers electrospun from the mixture of the poly(ethylene glycol) and PCL obtained with a conventional setup.<sup>156</sup> Mickova *et al.* reported the development of a nanofiber-liposome system for drug delivery. They tested the incorporation of liposomes containing the horseradish peroxidase drug with co-electrospinning and with coaxial electrospinning and demonstrated that the traditional setup does not preserve the integrity of the liposome which, in contrast, is well preserved. In this second case, the therapeutic activity of the encapsulated drug was demonstrated.<sup>158</sup>

Another approach to slow down the kinetics of release is the development of multilayer stacked nanofibers by the subsequent ES of two or more different solutions. Generally, these systems combine an initial fast release with a sustained release thanks to layers with different diffusion pathways and degradation behaviours. The versatility of layer by layer fiber deposition leads to a range of modifications and implementation to make it suitable also for multidrug delivery systems. Combining multiple treatments in different times plays a key role in chemotherapy for cancer treatment. Okuda and co-workers created tetra-layered drug-loaded nanofiber meshes for dual release. The construction was performed with a first drug-loaded layer, a second barrier mesh, a third drug-loaded layer and a final barrier mesh. An *in vitro* release assay demonstrated that the tetra-layered device can provide timed dual release of the respective drugs by tailoring the morphological features of each component mesh like the barrier mesh thickness.<sup>148–150,159</sup>



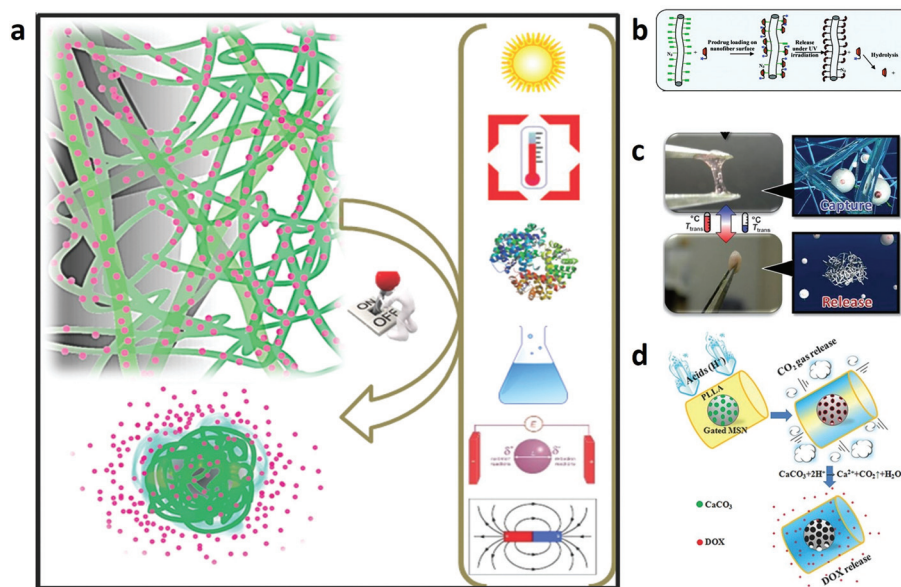


**Fig. 5** (a) Illustration of the mechanisms of on-demand drug release under biological, chemical, light, temperature, magnetic, and electric field stimuli.<sup>163</sup> (b) Schematic of the photocontrolled drug delivery based on the host–guest linkage on the photoresponsive nanofiber surface.<sup>161</sup> (c) A nanofiber web that captures and releases cells by switching to a hydrogel-like structure in response to temperature changes.<sup>164</sup> (d) A drug-loaded intelligent electrospun fiber mat which reacts only in pathological acidic environments by producing CO<sub>2</sub> gas with corresponding water penetration into the core of the fibers and rapid drug release.<sup>165</sup> Reproduced from ref. 161 with permission from American Chemical Society, copyright 2009; ref. 163 with permission from John Wiley and Sons, copyright 2014; ref. 164 with permission from John Wiley and Sons, copyright 2012; and ref. 165 with permission from John Wiley and Sons, copyright 2015.

**4.1.2. On-demand drug delivery fibers.** Since a number of polymers respond to external stimuli with consequent changes in their physical properties, a new frontier in drug delivery research is the development of smart polymeric fibers which release encapsulated drugs under the application of an external stimulus (temperature, light, magnetic field, and pH) for an on–off reversible switch (Fig. 5).<sup>160–162</sup>

In these systems, the drug is localized at a specific targeted area by internal or external forces and then activated. Recently, magnetic particles carrying drug molecules have been developed to target the drugs to specific sites in the body using external magnetic fields. Shortly after concentration in the targeted region, the drug molecules were gradually released, thus improving their therapeutic efficiency, while lowering the collateral toxic side effects on healthy cells or tissues.

For instance, Kim and co-workers reported temperature-responsive electrospun nanofibers for ‘on–off’ switchable release of dextran as a drug model.<sup>166</sup> Afterwards, Kim *et al.* designed smart nanofibers with bi-functional action by ES a chemically crosslinkable temperature-responsive polymer with magnetic nanoparticles and the anticancer drug (doxorubicin) for induction of skin cancer apoptosis. The nanofibers showed simultaneous heat generation and drug release in response to ‘on–off’ switching during an alternating magnetic field. The alternating magnetic field triggers self-generated heat from the incorporated nanoparticles and induces the deswelling of polymer networks in the nanofiber with consequent drug release. The double effects of the drug and heat resulted in successful treatment of human melanoma cells with about

70% of cancer cell mortality and this demonstrated their high potential as a manipulative hyperthermia material and a switchable drug release platform.<sup>160</sup>

Since cancer cells are known to secrete acids which reduce the pH to below 6.8, Zhao *et al.* reported in their work the production of a smart drug release system upon stimulation *via* pH changes. The system was realized by developing polymer fibers embedding drug loaded-mesoporous silica nanoparticles functionalized with CaCO<sub>3</sub> as an inorganic cap to control the opening of the pore entrances of the mesoporous silica nanoparticles inside the fibers. CaCO<sub>3</sub> starts to dissolve in Ca<sup>2+</sup> and CO<sub>2</sub> gas just after a reduction of the physiological pH in response to an acidic environment. During the release assay, the system demonstrated an improvement of the drug release amount as the pH decreased. Moreover, the *in vitro* tests with HeLa confirmed its cytotoxic ability due to the release of the drug in an acidic environment.<sup>165</sup>

#### 4.2. Electrospun fibers for gene delivery

RNA interference (RNAi) is a promising and powerful approach for cancer treatment. It is a mechanism by which double stranded RNAs mediate sequence-specific gene silencing, providing a new tool in the fight against cancer. On the other hand, uncontrolled transgene expression in non-target organs/sites/cells is problematic due to the high biological activities of transgene products. Furthermore, undesirable biodistribution of vectors leads to their loss and vector-dependent side effects. Thus, gene delivery systems that are targeted to specific organs/sites/cells are important for not only efficacy but also



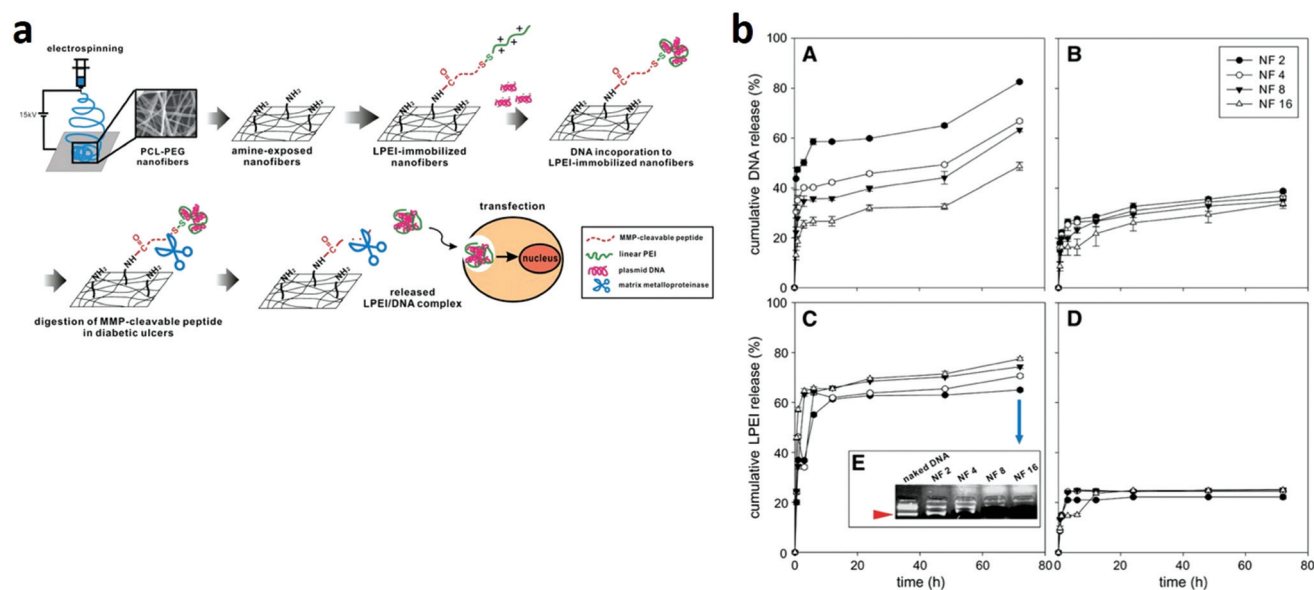


**Fig. 6** (a) Schematic diagram of an MMP-responsive electrospun nanofibrous matrix for gene delivery. (b) Release profiles of DNA (A and B) and LPEI (C and D) from the nanofibrous matrix in the presence of MMP-2.<sup>168</sup> Reproduced from ref. 168 with permission from Elsevier, copyright 2010.

**Table 3** List of polymer materials used for gene delivery by using ES nanofibers and respective cell lines used for gene delivery analysis

Material	Gene particle	Cell line	Ref.
PCL	pCMVb-GFP	3T3 (murine fibroblast cells)	171
	miRNA-145	HuH-7 (hepatocyte derived cellular carcinoma cells)	172
PCL-PEG	pEGFP-N1	NIH3T3 cells	168
PLLA	pGL3	COS-7 cells	14
PEI-PEG	pMSCV	HEK293 cells	173

Abbreviations: PCL – poly( $\epsilon$ -caprolactone), PEG – poly(ethylene glycol), PLLA – poly(L-lactic acid), and PEI – poly(ethylenimine).

safety. Since the initial study of Fang and Reneker, demonstrating the possibility of ES pure DNA nanofibers, the use of this technique for a variety of applications has truly increased to a significant extent.<sup>167</sup>

Electrospun nanofiber mediated siRNA delivery may serve as a potential alternative since the nanofiber can provide sustained long-term delivery at the tumour site (Fig. 6).<sup>168</sup>

In this regard, Achille and co-workers demonstrated the feasibility of loading into biodegradable fibers a bioactive plasmid encoding for short hairpin (sh) RNA against the cell cycle specific protein, Cdk2. The system led to the release of plasmid DNA during the fiber degradation, for over 21 days which suppressed the proliferation of MCF-7 breast cancer cells and affected their viability.<sup>169</sup> Lei and co-workers incorporated a RNAi plasmid designed to specifically suppress MMP-2, an essential proteinase regulating brain tumour invasion and angiogenesis in tumour cells, and a cytotoxic drug paclitaxel into PLGA based fibers to achieve a sustained release of both agents. It was found that DNA nanoparticles complexed with the gene carrier polyethylenimine and embedded in microfibers were able to inhibit MMP-2 mRNA and protein expression and, particularly, through an *in vivo* test on an intracranial xenograft tumour model in BALB/c nude mice it

was proved that the gene/drug dual delivery microfibers were able to impose significant tumour regression compared with single drug delivery microfibers and commercial drug treatment.<sup>170</sup> We have listed some of the ES nanofiber materials used for gene delivery in cancer cell lines (Table 3).

#### 4.3. Electrospun fibers for immunosensors/cancer screening

Evidence suggests that the detection and treatment of early stage cancer are essential in improving survival. However, early detection is difficult as it is usually asymptomatic until the disease has spread.<sup>174</sup> Results of previous studies highlighted that circulating antibodies to cancer associated antigens will likely be present in the early stages of disease and their detection might be the best way to identify early stage malignancies.<sup>175</sup>

Recent advances in nanoscience and nanotechnology have opened up new horizons for the development of biosensors of enhanced sensitivity, specificity, detection time, and low cost. Sensor miniaturization provides great versatility for incorporation into multiplexed, portable, wearable, and even implantable medical devices. The attractiveness of such nanomaterials relies not only on their ability to act as efficient and stabilizing platforms for the biosensing elements, but also on their small



size, large surface area, high reactivity, controlled morphology and structure, biocompatibility, and in some cases electrocatalytic properties. Structuring the transducer at the nano-scale contributes towards enlarging the overall surface available for bioreceptor immobilization. Incorporation of nanomaterials into the sensing layers is also often associated with higher mass transfer rates, acceleration and magnification of the transduction process, contributing to signal amplification and a faster biosensor response. In particular, fibers produced by ES are very interesting in this area since they can be chemically and physically decorated with bioactive molecules such as cell-recognizable ligands and provide a large surface area.<sup>176</sup> Sensing elements are principally enzymes, antibodies, and more scarcely DNA strands or aptamers and the mechanism of action is the electrochemical transduction.

Ali *et al.* reported the fabrication of an efficient, label-free, selective and highly reproducible immunosensor with unprecedented sensitivity (femto-molar) to detect a breast cancer biomarker for early diagnostics. Mesoporous zinc oxide nanofibers are synthesized by the ES technique and their fragments are electrophoretically deposited on an indium tin oxide glass substrate and conjugated *via* covalent or electrostatic interactions with a biomarker, the epidermal growth factor receptor 2. Label-free detection of the breast cancer biomarker using this point-of-care device is achieved by an electrochemical impedance technique that has high sensitivity ( $7.76 \text{ k}\Omega \mu\text{M}^{-1}$ ) and can detect a  $1 \text{ fM}$  ( $4.34 \times 10^{-5} \text{ ng mL}^{-1}$ ) concentration. The excellent impedimetric response of this immunosensor enables fast detection (128 s) in a wide detection test range ( $1.0 \text{ fM}$ – $0.5 \mu\text{M}$ ).<sup>177</sup>

Paul *et al.* reported a novel biosensor platform based on multiwalled carbon nanotube embedded zinc oxide nanowires for the ultrasensitive detection of carcinoma antigen-125. The system was synthesized by simple ES. The label-free detection

was performed by the differential voltammetry technique and it demonstrated excellent sensitivity ( $90.14 \mu\text{A (U mL}^{-1})^{-1} \text{ cm}^{-2}$ ) with a detection limit of  $0.00113 \text{ U mL}^{-1}$  concentration.<sup>178</sup> Soares *et al.* reported the fabrication of immunosensors based on nanostructured mats of electrospun nanofibers of polyamide 6 and poly(allylamine hydrochloride) coated with either multiwalled carbon nanotubes or gold nanoparticles, whose three-dimensional structure was suitable for the immobilization of anti-CA19-9 antibodies to detect the pancreatic cancer biomarker CA19-9. By using impedance spectroscopy, the sensing platform was able to detect CA19-9 with a sensitivity and detection limit of 1.84 and  $1.57 \text{ U mL}^{-1}$  for the nanostructured architectures containing multiwalled carbon nanotubes and gold nanoparticles, respectively. The high sensitivity and selectivity of the immunosensors were also explored in tests with blood serum from patients with distinct concentrations of CA19-9, for which the impedance spectral data were processed with a multidimensional projection technique. The robustness of the immunosensors in dealing with patient samples without suffering interference from analytes present in biological fluids is promising for a simple, effective diagnosis of pancreatic cancer at early stages.<sup>179</sup> More recently, a novel class of pH-sensing ES fiber scaffolds has been reported by embedding ratiometric pH sensing capsules directly within the lumen of electrospun organic fibers.<sup>180</sup> Upon proton-induced switching, the hybrid ratiometric organic fibers undergo optical changes that could be recorded with fluorescence detectors and correlated with the local proton concentration with micrometer-scale spatial resolution. Biocompatible ES fiber mats with pH sensing properties could be used for *in vivo* spatio-temporal measurements of the extracellular acidity of live cells, finding potential applications in drug screening and drug discovery for evaluating the efficacy of glycolysis inhibiting anti-cancer drugs in real time (Fig. 7).<sup>181,182</sup>

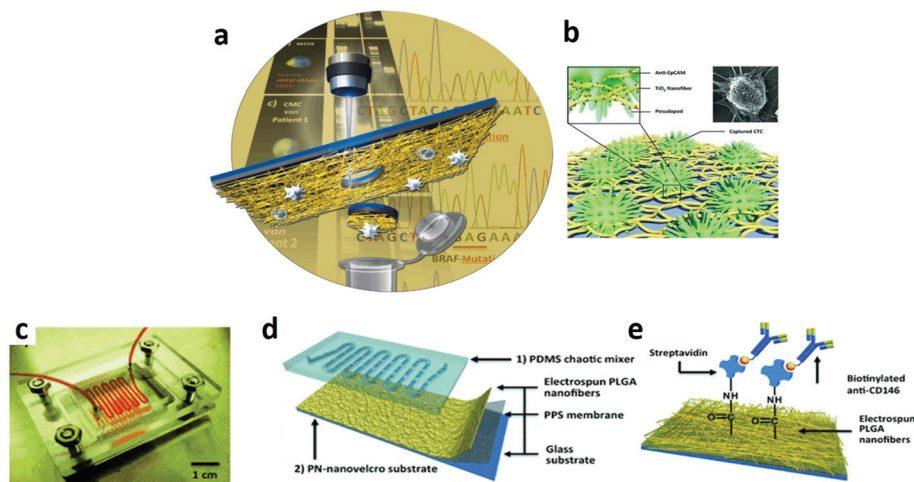


**Fig. 7** (a) A method to detect and isolate single circulating melanoma cells from normal white blood cells with a laser microdissection technique.<sup>181</sup> (b) A nanofiber platform  $\text{TiO}_2$ -based and biological cell-capture agent to capture circulating tumour cells.<sup>182</sup> (c) Picture of a nanostructured chip for melanoma cell isolation composed of (d) an overlaid PDMS chaotic mixer and a transparent nanovelcro substrate; (e) NHS chemistry is used to covalently anchor streptavidin for conjugation of biotinylated anti-CD146, a melanoma-specific antibody.<sup>181</sup> Reproduced from ref. 181 with permission from John Wiley and Sons, copyright 2013 and ref. 182 with permission from John Wiley and Sons, copyright 2012.



## 5. Conclusions

The high versatility, cost effectiveness and scalability of ES have been inspiring the design of novel strategies in cancer research. The use of electrospun scaffolds, such as polymer nanofibers that recapitulate the fibrous architecture of the native ECM environment, could help in the manufacture of xeno-free and highly controlled 3D *in vitro* tumour models for cell-based compound screening, mechanistic studies and pre-clinical drug discovery. Various approaches propose multifunctional and stimuli-responsive electrospun patches for topical release of therapeutics in a controlled and sustained way with improved therapeutic efficacy, reduced side effects and prolonged life expectancy of patients. Electrospun nanostructured mats also represent attractive sensor platforms to be used for fast diagnosis of cancers at early stages. Although numerous improvements have been achieved by employing electrospun scaffolds in cancer diagnosis and therapy, in depth *in vivo* studies are indispensable before use in clinical trials and medical device products.

## Conflicts of interest

There are no conflicts to declare.

## Acknowledgements

The authors gratefully acknowledge the ERC Starting Grant INTERCELLMED (project number 759959), the My First AIRC Grant (MFAG-2019, project number 22902), the FISIR-C.N.R., Tecnopolo di Nanotecnologia e Fotonica per la medicina di precisione (project number: B83B17000010001) and Tecnopolo per la medicina di precisione – Regione Puglia (project number: B84I18000540002).

## References

- 1 Y. M. Shin, M. M. Hohman, M. P. Brenner and G. C. Rutledge, *Polymer*, 2001, **42**, 09955–09967.
- 2 J. M. Deitzel, J. D. Kleinmeyer, J. K. Hirvonen and N. C. Beck Tan, *Polymer*, 2001, **42**, 8163–8170.
- 3 K. Y. Lee, L. Jeong, Y. O. Kang, S. J. Lee and W. H. Park, *Adv. Drug Delivery Rev.*, 2009, **61**, 1020–1032.
- 4 H. Homayoni, S. A. H. Ravandi and M. Valizadeh, *Carbohydr. Polym.*, 2009, **77**, 656–661.
- 5 D. H. Reneker and A. L. Yarin, *Polymer*, 2008, **49**, 2387–2425.
- 6 D. Deshwar and P. Chokshi, *Polymer*, 2017, **131**, 34–49.
- 7 T. J. Sill and H. A. von Recum, *Biomaterials*, 2008, **20**, 1989–2006.
- 8 E. D. Boland, J. A. Matthews, K. J. Pawlowski, D. G. Simpson, G. E. Wnek and G. L. Bowlin, *Front. Biosci.*, 2004, **9**, 1422–1432.
- 9 J. A. Matthews, G. E. Wnek, D. G. Simpson and G. L. Bowlin, *Biomacromolecules*, 2002, **3**, 32–238.
- 10 S. Eap, A. Ferrand, C. Mendoza-Palomares, A. Hébraud, J. F. Stoltz, D. Mainard, G. Schlatter and N. Benkirane-Jessel, in *Bio-Medical Materials and Engineering*, 2012, pp. 137–141.
- 11 N. J. Schaub, C. D. Johnson, B. Cooper and R. J. Gilbert, *J. Neurotrauma*, 2016, **33**, 1405–1415.
- 12 F. Ajallouei, H. Tavanai, J. Hilborn, O. Donzel-Gargand, K. Leifer, A. Wickham and A. Arpanaei, *BioMed Res. Int.*, 2014, 475280.
- 13 A. Nandakumar, H. Fernandes, J. De Boer, L. Moroni, P. Habibovic and C. A. Van Blitterswijk, *Macromol. Biosci.*, 2010, **10**, 1365–1373.
- 14 W. Chang, X. Mu, X. Zhu, G. Ma, C. Li, F. Xu and J. Nie, *Mater. Sci. Eng., C*, 2013, **33**, 4369–4376.
- 15 J. Erben, K. Pilarova, F. Sanetrik, J. Chvojka, V. Jencova, L. Blazkova, J. Havlicek, O. Novak, P. Mikes, E. Prosecka, D. Lukas and E. Kuzelova Kostakova, *Mater. Lett.*, 2015, **143**, 172–176.
- 16 F. Sharifi, S. M. Atyabi, D. Norouzi, M. Zandi, S. Irani and H. Bakhshi, *Int. J. Biol. Macromol.*, 2018, **115**, 243–248.
- 17 A. Wubneh, E. K. Tsekoura, C. Ayranci and H. Uludağ, *Acta Biomater.*, 2018, **80**, 1–30.
- 18 B. M. Baker, A. O. Gee, R. B. Metter, A. S. Nathan, R. A. Marklein, J. A. Burdick and R. L. Mauck, *Biomaterials*, 2008, **29**, 2348–2358.
- 19 M. T. Wolf, C. L. Dearth, S. B. Sonnenberg, E. G. Lobo and S. F. Badylak, *Adv. Drug Delivery Rev.*, 2015, **84**, 208–221.
- 20 O. Suwanton, S. Waleetorncheepsawat, N. Sanchavanakit, P. Pavasant, P. Cheepsunthorn, T. Bunaprasert and P. Supaphol, *Int. J. Biol. Macromol.*, 2007, **40**, 217–223.
- 21 H. Cao, T. Liu and S. Y. Chew, *Adv. Drug Delivery Rev.*, 2009, **61**, 1055–1064.
- 22 Y. M. Ju, J. S. Choi, A. Atala, J. J. Yoo and S. J. Lee, *Biomaterials*, 2010, **31**, 4313–4321.
- 23 H. Ahn, Y. M. Ju, H. Takahashi, D. F. Williams, J. J. Yoo, S. J. Lee, T. Okano and A. Atala, *Acta Biomater.*, 2015, **16**, 14–22.
- 24 P. Uttayarat, A. Perets, M. Li, P. Pimton, S. J. Stachelek, I. Alferiev, R. J. Composto, R. J. Levy and P. I. Lelkes, *Acta Biomater.*, 2010, **6**, 4229–4237.
- 25 M. B. Browning, D. Dempsey, V. Guiza, S. Becerra, J. Rivera, B. Russell, M. Höök, F. Clubb, M. Miller, T. Fossum, J. F. Dong, A. L. Bergeron, M. Hahn and E. Cosgriff-Hernandez, *Acta Biomater.*, 2012, **8**, 1010–1021.
- 26 S. Rayatpisheh, D. E. Heath, A. Shakouri, P. O. Rujitanaroj, S. Y. Chew and M. B. Chan-Park, *Biomaterials*, 2014, **35**, 2713–2719.
- 27 L. Poláková, J. Širc, R. Hobzová, A.-I. Cocârță and E. Heřmánková, *Int. J. Pharm.*, 2019, **558**, 268–283.
- 28 K. M. Kennedy, A. Bhaw-Luximon and D. Jhurry, *Acta Biomater.*, 2017, **50**, 41–55.
- 29 G. Jensen, C. Morrill and Y. Huang, *Acta Pharm. Sin. B*, 2018, **8**, 756–766.



- 30 E. Burdett, F. K. Kasper, A. G. Mikos and J. A. Ludwig, *Tissue Eng., Part B*, 2010, **63**, 351–359.
- 31 L. G. Griffith and G. Naughton, *Science*, 2002, **295**, 1009–1014.
- 32 O. Hartman, C. Zhang, E. L. Adams, M. C. Farach-Carson, N. J. Petrelli, B. D. Chase and J. F. Rabolt, *Biomacromolecules*, 2009, **10**, 2019–2032.
- 33 V. Agrahari, V. Agrahari, J. Meng and A. K. Mitra, in *Emerging Nanotechnologies for Diagnostics, Drug Delivery and Medical Devices*, 2017, pp. 189–215.
- 34 J. Wei, J. Hu, M. Li, Y. Chen and Y. Chen, *RSC Adv.*, 2014, **4**, 28011–28019.
- 35 J. Zhang, X. Wang, T. Liu, S. Liu and X. Jing, *Drug Delivery*, 2016, **23**, 784–790.
- 36 X. Xu, X. Chen, X. Xu, T. Lu, X. Wang, L. Yang and X. Jing, *J. Controlled Release*, 2006, **114**, 307–316.
- 37 S. Iqbal, M. H. Rashid, A. S. Arbab and M. Khan, *J. Biomed. Nanotechnol.*, 2017, **13**, 355–366.
- 38 P. Slemming-Adamsen, J. Song, M. Dong, F. Besenbacher and M. Chen, *Macromol. Mater. Eng.*, 2015, **300**, 1226–1231.
- 39 E. Yan, Y. Fan, Z. Sun, J. Gao, X. Hao, S. Pei, C. Wang, L. Sun and D. Zhang, *Mater. Sci. Eng., C*, 2014, **41**, 217–223.
- 40 J. Doshi and D. H. Reneker, *J. Electrostat.*, 1995, **35**, 151–160.
- 41 H. Zong, X. Xia, Y. Liang, S. Dai, A. Alsaedi, T. Hayat, F. Kong and J. H. Pan, *Mater. Sci. Eng., C*, 2018, **92**, 1075–1091.
- 42 Z.-M. Huang, Y.-Z. Zhang, M. Kotaki and S. Ramakrishna, *Compos. Sci. Technol.*, 2003, **63**, 2223–2253.
- 43 L. J. Chen, J. Der Liao, S. J. Lin, Y. J. Chuang and Y. S. Fu, *Polymer*, 2009, **50**, 3516–3521.
- 44 C. Su, C. Lu, H. Cao, F. Gao, J. Chang, Y. Li and C. He, *Mater. Lett.*, 2017, **204**, 8–11.
- 45 H. Y. Jian, S. V. Fridrikh and G. C. Rutledge, *Polymer*, 2006, **47**, 4789–4797.
- 46 N. Okutan, P. Terzi and F. Altay, *Food Hydrocolloids*, 2014, **39**, 19–26.
- 47 X.-F. Wu, Y. Salkovskiy and Y. A. Dzenis, *Appl. Phys. Lett.*, 2011, **98**, 223108.
- 48 O. S. Yördem, M. Papila and Y. Z. Menceloğlu, *Mater. Des.*, 2008, **29**, 34–44.
- 49 J. Zeng, H. Haoqing, A. Schaper, J. H. Wendorff and A. Greiner, *e-Polymers*, 2003, **3**, 102–110.
- 50 Y. Wu, L. A. Carnell and R. L. Clark, *Polymer*, 2007, **48**, 5653–5661.
- 51 D. Li, G. Ouyang, J. T. McCann and Y. Xia, *Nano Lett.*, 2005, **5**, 913–916.
- 52 D. Rodoplu and M. Mutlu, *J. Eng. Fibers Fabr.*, 2012, **7**, 118–123.
- 53 R. Sahay, V. Thavasi and S. Ramakrishna, *J. Nanomater.*, 2011, 1–17.
- 54 H. Pan, L. Li, L. Hu and X. Cui, *Polymer*, 2006, **47**, 4901–4904.
- 55 L. Wannatong, A. Sirivat and P. Supaphol, *Polym. Int.*, 2004, **53**, 1851–1859.
- 56 I. Hayati, A. I. Bailey and T. F. Tadros, *J. Colloid Interface Sci.*, 1987, **117**, 205–221.
- 57 H. Shin, S. Jo and A. G. Mikos, *Biomaterials*, 2003, **24**, 4353–4364.
- 58 F. Croisier and C. Jérôme, *Eur. Polym. J.*, 2013, **49**, 780–792.
- 59 E. K. Brenner, J. D. Schiffman, E. A. Thompson, L. J. Toth and C. L. Schauer, *Carbohydr. Polym.*, 2012, **87**, 926–929.
- 60 O. Hartman, C. Zhang, E. L. Adams, M. C. Farach-Carson, N. J. Petrelli, B. D. Chase and J. F. Rabolt, *Biomaterials*, 2010, **31**, 5700–5718.
- 61 C. J. Lovitt, T. B. Shelper and V. M. Avery, *Biology*, 2014, **3**, 345–367.
- 62 B. K. Jong, *Semin. Cancer Biol.*, 2005, **15**, 365–377.
- 63 H. Liu, J. Lin and K. Roy, *Biomaterials*, 2006, **27**, 5978–5989.
- 64 M. Turetta, F. Del Ben, G. Brisotto, E. Biscontin, M. Bulfoni, D. Cesselli, A. Colombatti, G. Scoles, G. Gigli and L. L. del Mercato, *Curr. Med. Chem.*, 2018, **25**, 4616–4637.
- 65 A. Polini, L. L. del Mercato, A. Barra, Y. S. Zhang, F. Calabi and G. Gigli, *Drug Discovery Today*, 2019, **24**, 517–525.
- 66 M. R. Carvalho, D. Barata, L. M. Teixeira, S. Giselsbrecht, R. L. Reis, J. M. Oliveira, R. Truckenmüller and P. Habibovic, *Sci. Adv.*, 2019, **5**, eaaw1317.
- 67 D. Barata, C. Van Blitterswijk and P. Habibovic, *Acta Biomater.*, 2016, **34**, 1–20.
- 68 T. P. Kraehenbuehl, R. Langer and L. S. Ferreira, *Nat. Methods*, 2011, **8**, 731–736.
- 69 D. Loessner, K. S. Stok, M. P. Lutolf, D. W. Huttmacher, J. A. Clements and S. C. Rizzi, *Biomaterials*, 2010, **31**, 8494–8506.
- 70 G. Rossi, A. Manfrin and M. P. Lutolf, *Nat. Rev. Genet.*, 2018, **19**, 671–687.
- 71 B. Alberts, A. Johnson, J. Lewis, M. Raff, K. Roberts and P. Walter, in *Molecular Biology of the Cell*, 2002, pp. 1131–1204.
- 72 M. Cavo, M. Caria, I. Pulsoni, F. Beltrame, M. Fato and S. Scaglione, *Sci. Rep.*, 2018, **8**, 5333.
- 73 M. Cavo, M. Fato, L. Peñuela, F. Beltrame, R. Raiteri and S. Scaglione, *Sci. Rep.*, 2016, **6**, 35367.
- 74 V. Kumar and S. Varghese, *Adv. Healthcare Mater.*, 2019, **8**, e1801198.
- 75 K. Chitcholtan, E. Asselin, S. Parent, P. H. Sykes and J. J. Evans, *Exp. Cell Res.*, 2013, **319**, 75–87.
- 76 T. E. Kim, C. G. Kim, J. S. Kim, S. Jin, S. Yoon, H. R. Bae, J.-H. Kim, Y. H. Jeong, J. Y. Kwak and K. J. Kim, *Int. J. Nanomed.*, 2016, **11**, 823–835.
- 77 S. Cai, H. Xu, Q. Jiang and Y. Yang, *Langmuir*, 2013, **29**, 2311–2318.
- 78 M. Rabionet, M. Yeste, T. Puig and J. Ciurana, *Polymers*, 2017, **9**, E328.
- 79 E. L. S. Fong, S. E. Lamhamedi-Cherradi, E. Burdett, V. Ramamoorthy, A. J. Lazar, F. K. Kasper, M. C. Farach-Carson, D. Vishwamitra, E. G. Demicco, B. A. Menegaz, H. M. Amin, A. G. Mikos and J. A. Ludwig, *Proc. Natl. Acad. Sci. U. S. A.*, 2013, **110**, 6500–6505.



- 80 A. A. Bulysheva, G. L. Bowlin, S. P. Petrova and W. A. Yeudall, *Biomed. Mater.*, 2013, **8**, 55009.
- 81 C. Ricci, C. Mota, S. Moscato, D. D'Alessandro, S. Ugel, S. Sartoris, V. Bronte, U. Boggi, D. Campani, N. Funel, L. Moroni and S. Danti, *Biomatter*, 2014, **4**, e955386.
- 82 H. Moghadas, M. S. Saidi, N. Kashaninejad, A. Kiyomarsioskouei and N.-T. Nguyen, *Biomed. Microdevices*, 2017, **19**, 74.
- 83 I. W. Y. Mak, N. Evaniew and M. Ghert, *Am. J. Transl. Res.*, 2014, **6**, 114–118.
- 84 G. Rijal and W. Li, *Biomaterials*, 2016, **81**, 135–156.
- 85 C. Frantz, K. M. Stewart and V. M. Weaver, *J. Cell Sci.*, 2010, **123**, 4195–4200.
- 86 J. A. DeQuach, V. Mezzano, A. Miglani, S. Lange, G. M. Keller, F. Sheikh and K. L. Christman, *PLoS One*, 2010, **5**, e13039.
- 87 C. Rianna, P. Kumar and M. Radmacher, *Semin. Cell Dev. Biol.*, 2018, **73**, 107–114.
- 88 N. F. Boyd, Q. Li, O. Melnichouk, E. Huszti, L. J. Martin, A. Gunasekara, G. Mawdsley, M. J. Yaffe and S. Minkin, *PLoS One*, 2014, **9**, e100937.
- 89 K. R. Levental, H. Yu, L. Kass, J. N. Lakins, M. Egeblad, J. T. Erler, S. F. T. Fong, K. Csiszar, A. Giaccia, W. Weninger, M. Yamauchi, D. L. Gasser and V. M. Weaver, *Cell*, 2009, **139**, 891–906.
- 90 C. A. Sherman-Baust, A. T. Weeraratna, L. B. A. Rangel, E. S. Pizer, K. R. Cho, D. R. Schwartz, T. Shock and P. J. Morin, *Cancer Cell*, 2003, **3**, 377–386.
- 91 T. Sethi, R. C. Rintoul, S. M. Moore, A. C. MacKinnon, D. Salter, C. Choo, E. R. Chilvers, I. Dransfield, S. C. Donnelly, R. Strieter and C. Haslett, *Nat. Med.*, 1999, **5**, 662–668.
- 92 A. Aung, V. Kumar, J. Theprungsirikul, S. K. Davey and S. Varghese, *Cancer Res.*, 2020, **80**, 263–275.
- 93 H. K. Kleinman and G. R. Martin, *Semin. Cancer Biol.*, 2005, **15**, 378–386.
- 94 G. Benton, H. K. Kleinman, J. George and I. Arnaoutova, *Int. J. Cancer*, 2011, **128**, 1751–1757.
- 95 V. Härmä, J. Virtanen, R. Mäkelä, A. Happonen, J. P. Mpindi, M. Knuutila, P. Kohonen, J. Lötjönen, O. Kallioniemi and M. Nees, *PLoS One*, 2010, **5**, e10431.
- 96 S. Chen, B. Liu, M. A. Carlson, A. F. Gombart, D. A. Reilly and J. Xie, *Nanomedicine*, 2017, **12**, 1335–1352.
- 97 J. Coburn, M. Gibson, P. A. Bandalini, C. Laird, H. Q. Mao, L. Moroni, D. Seliktar and J. Elisseeff, *Smart Struct. Syst.*, 2011, **7**, 213–222.
- 98 S. Chen, S. K. Boda, S. K. Batra, X. Li and J. Xie, *Adv. Healthcare Mater.*, 2018, **7**, 1701024.
- 99 R. L. Siegel, K. D. Miller and A. Jemal, *Ca-Cancer J. Clin.*, 2019, **69**, 7–34.
- 100 S. Saha, X. Duan, L. Wu, P. K. Lo, H. Chen and Q. Wang, *Langmuir*, 2012, **28**, 2028–2034.
- 101 Y. K. Girard, C. Wang, S. Ravi, M. C. Howell, J. Mallela, M. Alibrahim, R. Green, G. Hellermann, S. S. Mohapatra and S. S. Mohapatra, *PLoS One*, 2013, **8**, e75345.
- 102 J. Du, P. L. Che, Z. Y. Wang, U. Aich and K. J. Yarema, *Biomaterials*, 2011, **32**, 5427–5437.
- 103 K. Guiro, S. A. Patel, S. J. Greco, P. Rameshwar and T. L. Arinze, *PLoS One*, 2015, **10**, e0118724.
- 104 R. Siegel, D. Naishadham and A. Jemal, *Ca-Cancer J. Clin.*, 2012, **62**, 10–29.
- 105 C. Feig, A. Gopinathan, A. Neesse, D. S. Chan, N. Cook and D. A. Tuveson, *Clin. Cancer Res.*, 2012, **18**, 4266–4276.
- 106 Q. He, X. Wang, X. Zhang, H. Han, B. Han, J. Xu, K. Tang, Z. Fu and H. Yin, *Int. J. Nanomed.*, 2013, **8**, 1167–1176.
- 107 X. Wang, X. Zhang, Z. Fu and H. Yin, *J. Biotechnol.*, 2013, **166**, 166–173.
- 108 Y. Yamaguchi, D. Deng, Y. Sato, Y. Te Hou, R. Watanabe, K. Sasaki, M. Kawabe, E. Hirano and T. Morinaga, *Anticancer Res.*, 2013, **33**, 5301–5309.
- 109 J. A. Ludwig, S. E. Lamhamedi-Cherradi, H. Y. Lee, A. Naing and R. Benjamin, *Cancers*, 2011, **3**, 3029–3054.
- 110 M. Santoro, S. E. Lamhamedi-Cherradi, B. A. Menegaz, J. A. Ludwig and A. G. Mikos, *Proc. Natl. Acad. Sci. U. S. A.*, 2015, **112**, 10304–10309.
- 111 A. C. Bellail, S. B. Hunter, D. J. Brat, C. Tan and E. G. Van Meir, *Int. J. Biochem. Cell Biol.*, 2004, **36**, 1046–1069.
- 112 A. Jain, M. Betancur, G. D. Patel, C. M. Valmikinathan, V. J. Mukhatyar, A. Vakharia, S. B. Pai, B. Brahma, T. J. MacDonald and R. V. Bellamkonda, *Nat. Mater.*, 2014, **13**, 308–316.
- 113 M. Alfano, M. Nebuloni, R. Allevi, P. Zerbi, E. Longhi, R. Lucianò, I. Locatelli, A. Pecoraro, M. Indrieri, C. Speziali, C. Doglioni, P. Milani, F. Montorsi and A. Salonia, *Sci. Rep.*, 2016, **6**, 36128.
- 114 J. Hogge, D. Krasner, H. Nguyen, L. B. Harkless and D. G. Armstrong, *J. Am. Podiatr. Med. Assoc.*, 2000, **90**, 57–65.
- 115 Y. Wang, J. Qian, T. Liu, W. Xu, N. Zhao and A. Suo, *Mater. Sci. Eng., C*, 2017, **76**, 313–318.
- 116 D. H. Kim and D. Wirtz, *Proc. Natl. Acad. Sci. U. S. A.*, 2011, **108**, 6693–6694.
- 117 S. Ali, B. Nathalie, C. Judith and H. Dietmar, *Front. Bioeng. Biotechnol.*, 2016, **4**, 03011–03011.
- 118 A. Mantovani, *Nature*, 2009, **457**, 36–37.
- 119 A. S. Thakor and S. S. Gambhir, *Ca-Cancer J. Clin.*, 2013, **63**, 395–418.
- 120 M. S. Aslam, S. Naveed, A. Ahmed, Z. Abbas, I. Gull and M. A. Athar, *J. Cancer Ther.*, 2014, **05**, 817–822.
- 121 M. Zamani, M. P. Prabhakaran and S. Ramakrishna, *Int. J. Nanomed.*, 2013, **8**, 2997–3017.
- 122 R. Langer, *Science*, 1990, **249**, 1527–1533.
- 123 S. K. Vakkalanka, C. S. Brazel and N. A. Peppas, *J. Biomater. Sci., Polym. Ed.*, 1996, **8**, 119–129.
- 124 L. Brannon-Peppas, *Med. Plast. Biomater*, 1997, **4**, 34–44.
- 125 N. Bölgen, I. Vargel, P. Korkusuz, Y. Z. Menceloğlu and E. Pişkin, *J. Biomed. Mater. Res., Part B*, 2007, **81**, 530–543.
- 126 X. Xu, X. Chen, P. Ma, X. Wang and X. Jing, *Eur. J. Pharm. Biopharm.*, 2008, **70**, 165–170.
- 127 X. Xu, X. Chen, Z. Wang and X. Jing, *Eur. J. Pharm. Biopharm.*, 2009, **72**, 18–25.



- 128 J. W. Gatti, M. C. Smithgall, S. M. Paranjape, R. J. Rolfes and M. Paranjape, *Biomed. Microdevices*, 2013, **15**, 887–893.
- 129 T. Kowalczyk, A. Nowicka, D. Elbaum and T. A. Kowalewski, *Biomacromolecules*, 2008, **9**, 2087–2090.
- 130 K. Kanawung, K. Panitchanapan, S. O. Puangmalee, W. Utok, N. Kreua-Ongarjnuakool, R. Rangkupan, C. Meechaisue and P. Supaphol, *Polym. J.*, 2007, **39**, 369–378.
- 131 D. Puppi, A. M. Piras, N. Detta, D. Dinucci and F. Chiellini, *Acta Biomater.*, 2010, **6**, 1258–1268.
- 132 S. Y. Chew, R. Mi, A. Hoke and K. W. Leong, *Adv. Funct. Mater.*, 2007, **17**, 1288–1296.
- 133 H. Cao, X. Jiang, C. Chai and S. Y. Chew, *J. Controlled Release*, 2010, **144**, 203–212.
- 134 S. H. Ranganath and C. H. Wang, *Biomaterials*, 2008, **29**, 2996–3003.
- 135 S. Liu, G. Zhou, D. Liu, Z. Xie, Y. Huang, X. Wang, W. Wu and X. Jing, *J. Mater. Chem. B*, 2013, **1**, 101–109.
- 136 S. Zong, X. Wang, Y. Yang, W. Wu, H. Li, Y. Ma, W. Lin, T. Sun, Y. Huang, Z. Xie, Y. Yue, S. Liu and X. Jing, *Eur. J. Pharm. Biopharm.*, 2015, **93**, 127–135.
- 137 R. Ramachandran, V. R. Junnuthula, G. S. Gowd, A. Ashokan, J. Thomas, R. Peethambaran, A. Thomas, A. K. K. Unni, D. Panikar, S. V. Nair and M. Koyakutty, *Sci. Rep.*, 2017, **7**, 43271.
- 138 J. Zeng, X. Xu, X. Chen, Q. Liang, X. Bian, L. Yang and X. Jing, *J. Controlled Release*, 2003, **92**, 227–231.
- 139 K. Kim, Y. K. Luu, C. Chang, D. Fang, B. S. Hsiao, B. Chu and M. Hadjiargyrou, *J. Controlled Release*, 2004, **98**, 47–56.
- 140 S. Y. Chew, J. Wen, E. K. F. Yim and K. W. Leong, *Biomacromolecules*, 2005, **5**, 2017–2024.
- 141 J. A. Henry, M. Simonet, A. Pandit and P. Neuenschwander, *J. Biomed. Mater. Res., Part A*, 2007, **82**, 669–679.
- 142 K. Kim, M. Yu, X. Zong, J. Chiu, D. Fang, Y. S. Seo, B. S. Hsiao, B. Chu and M. Hadjiargyrou, *Biomaterials*, 2003, **24**, 4977–4985.
- 143 X. Zhou, L. Chen, W. Wang, Y. Jia, A. Chang, X. Mo, H. Wang and C. He, *RSC Adv.*, 2015, **5**, 65897–65904.
- 144 X. Zhang, X. Xie, H. Wang, J. Zhang, B. Pan and Y. Xie, *J. Am. Chem. Soc.*, 2013, **135**, 18–21.
- 145 B. Song, C. Wu and J. Chang, *Acta Biomater.*, 2012, **8**, 1901–1907.
- 146 F. Zheng, S. Wang, S. Wen, M. Shen, M. Zhu and X. Shi, *Biomaterials*, 2013, **34**, 1402–1412.
- 147 P. Balakrishnan, L. Gardella, M. Forouharshad, T. Pellegrino and O. Monticelli, *Colloids Surf., B*, 2018, **161**, 488–496.
- 148 M. Yoshida, R. Langer, A. Lendlein and J. Lahann, *Polym. Rev.*, 2006, **46**, 347–375.
- 149 M. Deminsky, V. Jivotov, B. Potapkin and V. Rusanov, *Pure Appl. Chem.*, 2002, **74**, 413–418.
- 150 Y. Il Cho, J. S. Choi, S. Y. Jeong and H. S. Yoo, *Acta Biomater.*, 2010, **6**, 4725–4733.
- 151 F. Zomer Volpato, J. Almodóvar, K. Erickson, K. C. Popat, C. Migliaresi and M. J. Kipper, *Acta Biomater.*, 2012, **8**, 1551–1559.
- 152 J. S. Im, J. Yun, Y. M. Lim, H. Il Kim and Y. S. Lee, *Acta Biomater.*, 2010, **6**, 102–109.
- 153 G. Ma, Y. Liu, C. Peng, D. Fang, B. He and J. Nie, *Carbohydr. Polym.*, 2011, **86**, 505–512.
- 154 P. Zhao, H. Jiang, H. Pan, K. Zhu and W. Chen, *J. Biomed. Mater. Res., Part A*, 2007, **83**, 372–382.
- 155 H. Jiang, Y. Hu, Y. Li, P. Zhao, K. Zhu and W. Chen, *J. Controlled Release*, 2005, **108**, 237–243.
- 156 Y. Z. Zhang, X. Wang, Y. Feng, J. Li, C. T. Lim and S. Ramakrishna, *Biomacromolecules*, 2006, **7**, 1049–1057.
- 157 A. Saraf, L. S. Baggett, R. M. Raphael, F. K. Kasper and A. G. Mikos, *J. Controlled Release*, 2010, **143**, 95–103.
- 158 A. Mickova, M. Buzgo, O. Benada, M. Rampichova, Z. Fisar, E. Filova, M. Tesarova, D. Lukas and E. Amler, *Biomacromolecules*, 2012, **13**, 952–962.
- 159 T. Okuda, K. Tominaga and S. Kidoaki, *J. Controlled Release*, 2010, **143**, 258–264.
- 160 Y. J. Kim, M. Ebara and T. Aoyagi, *Adv. Funct. Mater.*, 2013, **23**, 5753–5761.
- 161 G. D. Fu, L. Q. Xu, F. Yao, G. L. Li and E. T. Kang, *ACS Appl. Mater. Interfaces*, 2009, **1**, 2424–2427.
- 162 S. Kato, K. Ozasa, M. Maeda, Y. Tanno, S. Tamaki, M. Higuchi-Takeuchi, K. Numata, Y. Kodama, M. Sato, K. Toyooka and T. Shinomura, *Plant J.*, 2019, 14576.
- 163 M. Chen, Y. F. Li and F. Besenbacher, *Adv. Healthcare Mater.*, 2014, **3**, 1721–1732.
- 164 Y. J. Kim, M. Ebara and T. Aoyagi, *Angew. Chem., Int. Ed.*, 2012, **51**, 10537–10541.
- 165 X. Zhao, Z. Yuan, L. Yildirimer, J. Zhao, Z. Y. Lin, Z. Cao, G. Pan and W. Cui, *Small*, 2015, **11**, 4284–4291.
- 166 Y. J. Kim, M. Ebara and T. Aoyagi, *Sci. Technol. Adv. Mater.*, 2012, **13**, 064203.
- 167 X. Fang and D. H. Reneker, *J. Macromol. Sci., Part B: Phys.*, 1997, **36**, 169–173.
- 168 H. S. Kim and H. S. Yoo, *J. Controlled Release*, 2010, **145**, 264–271.
- 169 C. Achille, S. Sundaresh, B. Chu and M. Hadjiargyrou, *PLoS One*, 2012, **7**, e52356.
- 170 C. Lei, Y. Cui, L. Zheng, P. Kah-Hoe Chow and C. H. Wang, *Biomaterials*, 2013, **34**, 7483–7494.
- 171 J. Jiang, M. Ceylan, Y. Zheng, L. Yao, R. Asmatulu and S.-Y. Yang.
- 172 H.-L. Che, H. J. Lee, K. Uto, M. Ebara, W. J. Kim, T. Aoyagi and I.-K. Park, *J. Nanosci. Nanotechnol.*, 2015, **15**, 7971–7975.
- 173 J. Zhang, Y. Duan, D. Wei, L. Wang, H. Wang, Z. Gu and D. Kong, *J. Biomed. Mater. Res., Part A*, 2011, **96**, 212–220.
- 174 U. Menon and I. J. Jacobs, in *International Journal of Gynecological Cancer*, 2001, pp. 3–6.
- 175 I. Kirman, G. F. Kalantarov, L. I. Lobel, H. Hibshoosh, A. Estabrook, R. Canfield and I. Trakht, *Hybridoma Hybridomics*, 2002, **21**, 405–414.



- 176 H. Y. Son, J. H. Ryu, H. Lee and Y. S. Nam, *ACS Appl. Mater. Interfaces*, 2013, **5**, 6381–6390.
- 177 M. A. Ali, K. Mondal, C. Singh, B. Dhar Malhotra and A. Sharma, *Nanoscale*, 2015, **7**, 7234–7245.
- 178 K. B. Paul, V. Singh, S. R. K. Vanjari and S. G. Singh, *Biosens. Bioelectron.*, 2017, **88**, 144–152.
- 179 J. C. Soares, L. E. O. Iwaki, A. C. Soares, V. C. Rodrigues, M. E. Melendez, J. H. T. G. Fregnani, R. M. Reis, A. L. Carvalho, D. S. Correa and O. N. Oliveira, *ACS Omega*, 2017, **2**, 6975–6983.
- 180 L. L. del Mercato, M. Moffa, R. Rinaldi and D. Pisignano, *Small*, 2015, **22**, 6417–6424.
- 181 S. Hou, L. Zhao, Q. Shen, J. Yu, C. Ng, X. Kong, D. Wu, M. Song, X. Shi, X. Xu, W.-H. H. Ouyang, R. He, X.-Z. Zhao, T. Lee, F. C. Brunicardi, M. A. Garcia, A. Ribas, R. S. Lo and H.-R. R. Tseng, *Angew. Chem., Int. Ed.*, 2013, **52**, 3379–3383.
- 182 N. Zhang, Y. Deng, Q. Tai, B. Cheng, L. Zhao, Q. Shen, R. He, L. Hong, W. Liu, S. Guo, K. Liu, H. R. Tseng, B. Xiong and X. Z. Zhao, *Adv. Mater.*, 2012, **24**, 2756–2760.

